2018

A Figure of Merit Approach to Quantifying Dye Degradation in Film Based Reactors

Atheer Hadi Abed Al-Musawi
University of Wollongong

UNIVERSITY
OF WOLLONGONG
AUSTRALIA

A Figure of Merit Approach to Quantifying Dye Degradation in Film Based Reactors

Atheer Hadi Abed Al-Musawi

This thesis is presented as part of the requirement for the conferral of the degree:

Master of Philosophy

The University of Wollongong

School of Chemistry

August 2018

Abstract

Dyes are organic compounds produced from the dyeing and printing processes used in the textile manufacturer. Some dyes are categorized as toxic to the environment when discharged; therefore, dye removal techniques are required. MB is a dye of a low toxicity compared to the other dyes used by numerous studies as a model dye for compounds of similar structure to investigate its degradation. Heterogenous photocatalysis has been utilized for successful removal of these dyes using semiconductors as photocatalysts. Semiconductors are extensively employed for dyes removal due to promising properties in this field. Herein, titanium dioxide (TiO_2 P25) and bismuth vanadate ($BiVO_4$) have been applied as important photocatalysts to study the degradation of MB model dye. TiO_2 and $BiVO_4$ were designed in film style and left under solar simulation equipment for a given time to monitor their photocatalytic rates activity towards MB degradation. The primary focus of the current study represented by studying the effect of different factors on the film's performance including films thickness and size, reactor volume, temperature, light intensity, and initial dye concentration to develop figure of merit. My approach for developing a figure of merit was done by varying one of the pre-mentioned factors while keeping the others constant. The outcomes of carried out

investigations showed an increased degradation rate by increasing films size and thickness, temperature, and light intensity. However, increasing reactor volume indicated a decreased rate constant for MB degradation.

Acknowledgments

I would like to thank my principle supervisor, Professor. Jun Chen, for his support and guidelines through my thesis writing and lab work. I am also grateful to Dr. Andrew Nattestad for being patient with me and valuable assistance and suggestions to my thesis chapters and scientific work. Deep thanks to Professor. Gordon Wallace for studying at the Intelligent Polymer Research Institute (IPRI).

I would like to thank the ARC Centre of Excellence for Electromaterials Science (ACES), the Australian National Fabrication Facility (ANFF) at the University of Wollongong (Australia) for their equipment and supplements. To my wife Dr. Wed Al-graiti, and my children: Zain Alabideen, Ahmed, and the newborn baby Rayan. To my priceless and great parents.

Certification

I, Atheer Al-Musawi, declare that this thesis submitted in fulfilment of the requirements for the conferral of the degree Master, from the University of Wollongong, is wholly my own work unless otherwise referenced or acknowledged. This document has not been submitted for qualifications at any other academic institution.

_____

Atheer Al-Musawi

August 2018

List of Abbreviations

VB	VALENCE BAND
CB	CONDUCTION BAND
TiO_2	TITANIUM DIOXIDE
$BiVO_4$	BISMUTH VANADATE
UV	ULTRAVIOLET
POP_S	PERSISTENT ORGANIC POLLUTANTS
MB	METHYLENE BLUE
H_2	Hydrogen
O_2	OXYGEN
h^+	HOLES
e^-	ELECTRONS
AOP	ADVANCED OXIDATION PROCESS
LH	LANGMUIR HINSHELWOOD
$OH^\bullet$	HYDROXYL RADICALS
CO_2	CARBON DIOXIDE
HNO_3	NITRIC ACID
IPRI	INTELLIGENT POLYMER RESEARCH INSTITUTE
µM	MICROMOLAR
cm	CENTIMETRE
E	POTENTIAL

Table of Contents

Table of Contents

List of Figures

List of Table

CHAPTER-1-

INTRODUCTION AND LITERATURE REVIEW

1.1. Background

Established industry sectors, in particular, clothing and leather manufacturers have reached an important commercial stage in recent years [1, 2]. Textile industries have been in more demand with increases in population, resulting in greater consumption of clothing. In addition, the strong growth of textile production industries is based on an increased desire for natural and artificial fibres, like cotton and nylon, respectively [3]. Organic and inorganic compounds discharged into water from such industries can be harmful to animal and plant life and may also be a threat to human beings [4]. The production of textiles requires various stages, including but not limited to, spinning, weaving, bleaching and dyeing. Dyeing and printing are significant and extremely popular processes used in textile manufacturing [5]. Some by-products of textile dyeing are hazardous substances (compounds) which can be categorised as highly toxic and/or non-biodegradable chemicals. These are often discharged into surface waters. The production of textiles is extremely water intensive, with around 200 L to produce 1 kg of textile reported [6]. The amount of water consumed varies for each industry. Water discharged from textile industries is subject to legislative standards because of the potential to contain huge amounts of chemicals harmful to human health. Contaminants of concern for wastewater are monitored as follows: colours, chemicals, dissolved solids, chemical oxygen demand (COD), biological oxygen demand (BOD), and metals like Cr, As, Cu and Zn which cannot be degraded [7, 8]. Coloured dyes, are considered important pollutants [3].

Even though many conventional methods have been used to remove dyes from wastewater, these were not cost effective, needing extended time

periods and ultimately releasing non-biodegradable products [9]. Therefore, finding a new and environmentally friendly method suitable for studying degradation and removal of dyes is required. Heterogeneous photocatalysis has been extensively used for the successful removal of dyes in the last few decades, as described in thousands of publications [10]. This process ~~refers~~ is referred to a precipitated (accelerated) photoreaction carried out by a catalyst [11]. Major applications of photocatalysis include water splitting and water purification from low levels of pollutants, by solar energy [11]. For example, MB and rhodamine B have been used as model dyes to investigate remediation of water systems from compounds that have similar optical and chemical properties.

Semiconductor photocatalysis offers great advantages in applications for waste water treatment [10, 12] . In addition, the incorporation of nanoscale materials has also demonstrated promise. TiO_2-based nanomaterial was found to have extreme reactivity for photochemical reactions [13]. The importance of TiO_2 can be attributed to its high chemical stability and non-toxic properties [14]. The discovery of nano-TiO_2 as a catalyst in the 1970s was associated with stimulation by UV radiation [15]. The rate constant or percentage removal of dyes after a specific time is used to study the degradation of dyes.

1.2. Organic Water Pollutants

In recent years, persistent organic pollutants (POPs), such as extremely toxic pesticides, heavy metals and industrial chemicals, have created severe problems in the modern world. Firstly, they are highly resistant to degradation, hence they persist in water environments long-term (years and sometimes, decades). Also, industrial chemicals are able to be transported for extended

periods. Persistent POPs can be absorbed into aquatic life forms which results in bioaccumulation and bioconcentration up the food chain. Furthermore, the growth of photosynthetic aquatic biota can be inhibited by reduced sunlight penetration in water. In addition to ecosystem damage, there is the potential for a huge impact on human health [16]. Numerous types of organic pollutants found in water are considered illegal chemical compounds, as their use has been banned or restricted. Thousands of different POPs exist in wastewater due to industrial manufacture. There are many traditional methods to remove each type of organic pollutants from wastewater. The focus of this chapter is remediation of wastewater from synthetic dyes.

1.2.1. Organic Dyes and industry applications

A huge number of organic dyes have been used in the textile industry as well as in other industries like cosmetics, plastics, and pharmaceuticals [17]. Dyes are generally identified as coloured materials which can exist as soluble substances or those that release colour through light by selective absorption. Moreover, chemical and physical properties of dyes develop an interaction between substances and light with colour as the result [18]. It has been estimated that 90% of the 10^7 Kg of dye consumed per year in the textile industry is used on fabrics. 10^6 Kg of dye is disposed into wastewater from textile industries each year which causes a severe environmental problem [19].

Dyes are extensively used in numerous fields including leather treatment, paper industries, food, medication, cosmetics, agrarian and scientific research [20].

Generally, dyes are classified based on their origin and dye structure into the azo dyes, anionic, cationic and non-ionic dyes. MB is a cationic dye which

is assumed to be indicative of other azo dye degradation MB is used by many researches dating back to Honda et.al. 1977 [21].

MB

MB is a dye belongs to the xanthine family has been the focus of many photocatalytic studies, owing to its water dispersibility, non-biodegradability and high stability. Wastewater discharged from dyeing cotton contains large amounts of MB. Therefore, wastewater needs to be treated to avoid the effects of toxic organic compounds [22]. Notably, MB has low toxicity compared to other dyes of similar structure. Hence, it been selected for studying the photocatalytic performance of semiconductors.

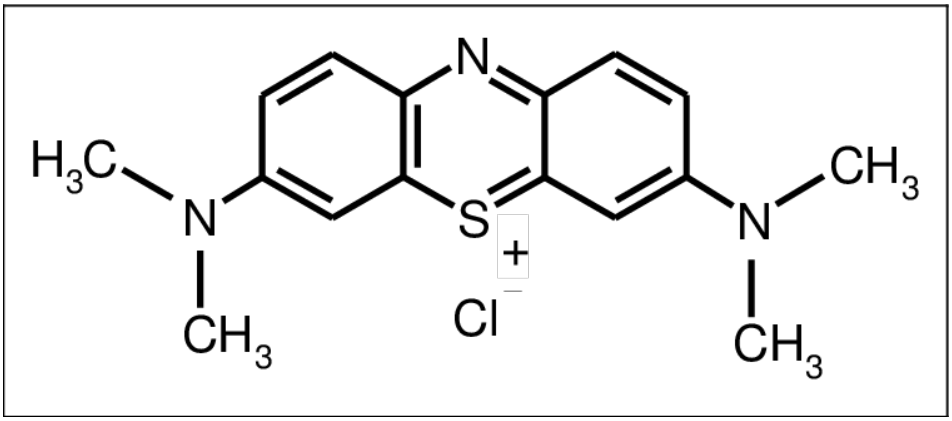

Figure 1.1 Chemical structure of MB dye [23]

MB is heterocyclic with aromatic rings (Figure 1.1). The molecular structure of MB is $C_{16}H_{18}N_3SCl$ with 319.09 $g.mol^{-1}$ molecular weight and (45 µM MB solution has absorption at 664 nm wavelength absorption [24]. The IUPAC name of MB is (Dimethylamino)-phenazathionium chloride or Tetramethylthionine chloride] [25]. Physical and chemical properties of MB are listed in Table 1.1.

Table 1. 1 Physical and chemical properties of MB [26]

Properties of MB	Values
Molecular weight	319.09 g/mol
pH	3 (10g/L H_2O)
Boiling point	No data - Decomposes
Melting point	180° C
Solubility in water	35.5 g/L
Molecular formula	$C_{16}H_{18}N_3ClS$

MB is frequently used as a model for the elimination of basic dye by adsorption [27] and electrodegradation [28]. Conversely, oxidized structures of MB are much more stable. MB can be instantly re-formed when its oxidized structure is reduced in acidic conditions. Figure 1.2 illustrates the photocatalytic degradation mechanism of MB starting with the demethylation step, followed by deamination to break the MB rings at the bonds C-S=$^{+}$C. By-products resulting from breaking the ring such as phenylamine and phenol would be oxidized and finally transformed into H_2O, CO_2 and NO_2 and SO_4^{-2}[29].

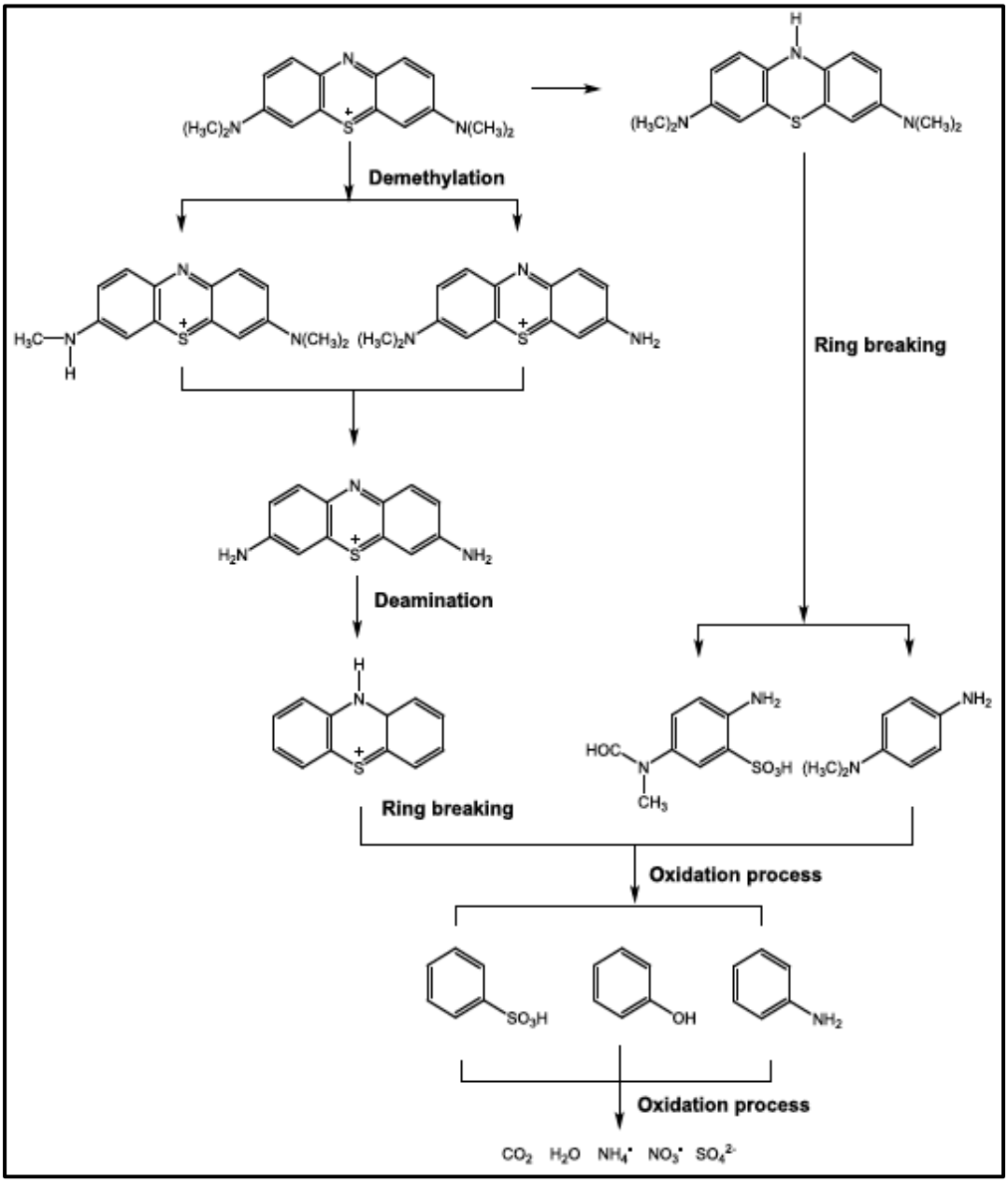

Figure 1.2 Photocatalytic degradation pathway of MB based on [30]

1.3. Dye Removal Techniques

1.3.1. Traditional Techniques

Numerous techniques have been successively applied to the elimination of organic dyes from wastewater to reduce their ecological effects. These techniques can be classified into physical, chemical and biological treatments.

There are several factors which reduce the effectiveness of these methods such as the remarkable stability of the chemical structure of synthetic dyes [31].

Physical methods including nanofiltration [32], electrodialysis [33] and reverse osmosis [34] added to sorption technologies have all been used for removal of dye from the aquatic environment. These methods have excellent abilities to eliminate colours from wastewater, however, they cannot destroy the dye molecules. As a result, vast amounts of dye would be accumulated, and this would require a process for treating the dye. The use of chemical and biological methods has been widely investigated. Coagulation and flocculation used with filtration plus traditional oxidation methods, precipitation, enzyme utilisation and anaerobic microbial procedures have all been employed for textile dye removal from wastewater to reduce environmental damage. Although these techniques had potentially suitable properties for remediation, textile dyes in wastewater displayed high chemical stability which prevented traditional procedures and technologies from being effective. Moreover, some of these were expensive or required specialist teams to operate them [35]. Others were ineffective due to interference from other molecules, unsuitable pH or temperature or had other operational problems.

1.3.2. Adsorption

The discovery of the “adsorption” process goes back to the 18th century when first reported by Kayser [36]. This process involves a colour removal phenomenon when liquid and solid phases, or substances, are present together. The liquid phase (usually a dye), identified as “adsorbate”, is distributed around a solid substance, “adsorbent”, then aggregates on the solid

surface via chemical or physical bonds. The two types of adsorption described are chemical adsorption (chemisorption) and physical adsorption. In such processes, adsorbates and adsorbents would undergo chemical or physical interactions, based on forming covalent or non-covalent bonds, respectively.

Dye adsorption may be enhanced based on dye properties and surface chemistry of the adsorbent [37]. In order to achieve successful dye elimination and effective water treatment, the materials selected for adsorption should be highly porous. Activated carbon, for example, is a good candidate for such applications. It has pore sizes which range from Macropores (bigger than 25 nm) and Mesopores (started from 1 up to 25 nm) to Micropores (less than 1 nm) based on manufacture [37]. In addition to pore size, low cost, high surface area and availability of the material are all important when choosing an adsorbent.

As adsorption will always occur, therefore, good experimental practice for photo-degradation involves a preliminary step with the dye and catalyst held in the dark to attain an adsorption-desorption equilibrium. Otherwise, not doing this will convolute results and make analysis more difficult.

1.3.3. Advanced Oxidation Processes (AOPs)

Aforementioned drawbacks to traditional treatment methods can be overcome by using the new generation of removal techniques known as advanced oxidation processes (AOPs). The mechanism of the AOP method includes the creation of free radicals, in particular, hydroxyl radicals, exceptional oxidizing agents which eliminate the organic contaminants and give ultimate products CO_2, H_2O, NO_X, SO_X, and others depending on dye structure. A specific example for AOP are UV photolysis ,UV/H_2O_2 systems

1.3.3.1. Photocatalysis

Photocatalysis is a method used to accelerate chemical reactions by using catalysts which require light. A photocatalyst is a specific material with the ability to absorb light and generate free electron-hole pairs, which then go on to generate radical species. Photocatalysis can be divided into homogeneous and heterogenous reactions.

Important features of a photocatalytic system are: large surface area; high stability; re-utilization; having the required band gap and morphology. A number of metal oxides have been utilised for photocatalytic reactions including titanium dioxide and bismuth-vanadate[37]. These oxides enable light absorption to introduce a suitable charge separation that allows positive hole formation able to be utilised as oxidants for organic substances. The source for metal oxide activation could be UV light and/or visible light exciting the electrons to transfer from the lower band (valence band) VB to the upper band (conduction band) CB to create the electron/hole pair. This pair can oxidize and/or reduce the adsorbed substances on the surface of the photocatalyst. The photocatalytic activity of applied metal oxides is governed by the generation of •OH radicals and O_2^- anions. These radicals and anions participate in the degradation reaction of pollutants to convert them into harmless products.

Photocatalysis is used in several applications, one of which is photocatalytic water splitting. This process can meet specific requirements such as high energy production in the form of abundant, storable Hydrogen to be utilised as fuel, without the release of pollutants. Although water splitting can be carried out by three different approaches, including thermochemical,

photobiological, and photocatalytic processes, the latter proved to be more advantageous than the others due to cost effectiveness, control over H_2 and O_2 separation and production and the ability to use different reactor sizes [38].

1.4. Semiconductors used for Photocatalysis

Semiconductors are materials have an electrical resistivity between 10^{-2} to 10^{9} Ohm cm^{-1}. They are found in a wide range of crystal configurations and classified as elements or compounds. A band gap (E_g) is a distinctive property of a semiconductor. It shows the difference in energy between top and bottom levels of energy called the valence band (VB) and conduction band (CB) as following:

$E_g = CB - VB$

When the surface of a semiconductor is exposed to sufficient photon energy, an electron (e^-) would be shifted from the CB to the CB to generate a hole (h^+) in the lowest level, this process is called exciton generation and it needs a minimum energy to happen:

$X + hv \rightleftharpoons h^+ + e^-$ X= semicondutor , hv= photon Energy

In this way, the promoted electron and the created hole would behave like a reducing agent and an oxidizing agent respectively:

$A + e^- \rightleftharpoons \bullet A^-$ A: acceptor

$D + h^+ \rightleftharpoons \bullet D^+$ D: donor

As a result, the oxidation power can induce the water oxidation process to produce a hydroxyl radical:

$H_2O + h^+ \rightleftharpoons \bullet OH + H^+$ Band gap= 4.92 eV [39]

On the other hand, oxygen atoms would be reduced by the electron in the CB to introduce ions with highly oxidant energy ($\bullet O_2^-$). This ion enables fast decomposition of organic compounds through the oxidation-reduction process is[39]: $O_2 + e^- \rightleftharpoons \bullet O_2^-$

Transfer the electron from the VB to CB will create free electron in the CB and a hole in the VB, when the free electron in CB and a hole in the VB meet and annihilate each other, the process called recombination of electron-hole pairs. The band gap is the minimal energy difference between the top edge of the VB and the lower edge of the CB, when the difference has the same value of momentum then it's called a direct bandgap semiconductor, however, when the minimum energy in the CB and the maximum energy in the VB occur at different values of the crystal momentum it's called Indirect-band-gap[40].

There are many different types of semiconductor materials have already been studied and reported in the literatures [41- 43] [44].

1.4.1. Titanium Dioxide (TiO_2)

TiO_2 has been shown to be an effective catalyst , according to outstanding optical and electronic properties, photoactivity, high chemical stability, stable in water, nontoxic, reusable, band gap of 3.2 eV applicable to the UV-region, eco-friendly, and low-cost material [45-47]. It has been applied for environmental purification, self-cleaning surfaces, sterilization and energy/conversion applications [46, 48]. Three well-known crystallographic structure of TiO_2 which are anatase, rutile, and brookite. Anatase and rutile are

tetragonal crystals whereas brookite is an orthorhombic crystal [47]. In fact, anatase and rutile are mostly used phases of TiO_2 as anatase has higher bandgap = 3.2 eV absorbing light near the UV range while rutile's bandgap = 3.0 eV absorbs visible light [47]. Thermodynamical stability of rutile is significant, whereas anatase is kinetically stable and can transform to rutile at high temperature. The rapid oxidizing behavior of anatase-TiO_2 is particularly useful for breaking down organic and inorganic pollutants.

Semiconductors can be used in powder-based suspensions and films for dye degradation in pristine and composite structures [50]. Study applied three types of TiO_2 powders (P25, UV100, and PC500) for the photodegradation of chromotrope 2B dye. P25 demonstrated the highest degradation rate in comparison to the other TiO_2 materials [51]. TiO_2 P25 was also used in a different study of photocatalytic degradation of MB dye. The results were sound and accurately revealed how the reaction rate can be influenced by catalyst and dye concentrations [52]. Significant photocatalytic activity of MB on a P25 surface was demonstrated by another study using TiO_2 nanoparticles created via thermal decomposition of TTIP (titanium tetraisopropoxide) [53].

The mechanism of MB photodegradation by TiO_2 can be explained in figure (1.3). When UV irradiation (3.2 eV or more) hits TiO_2, an electron will transfer from the (VB) to the (CB) leaving a hole (h_{VB}) behind. The positive hole can oxidize MB molecule (or hydroxide ions) adsorbed on the surface of TiO_2 particles to produce hydroxyl radicals. The electrons of the CB can react with the oxygen to produce superoxide radical anions. Then, hydroxyl radicals and superoxide radicals react with MB over few intermediate steps and give the final products CO_2 and H_2O.

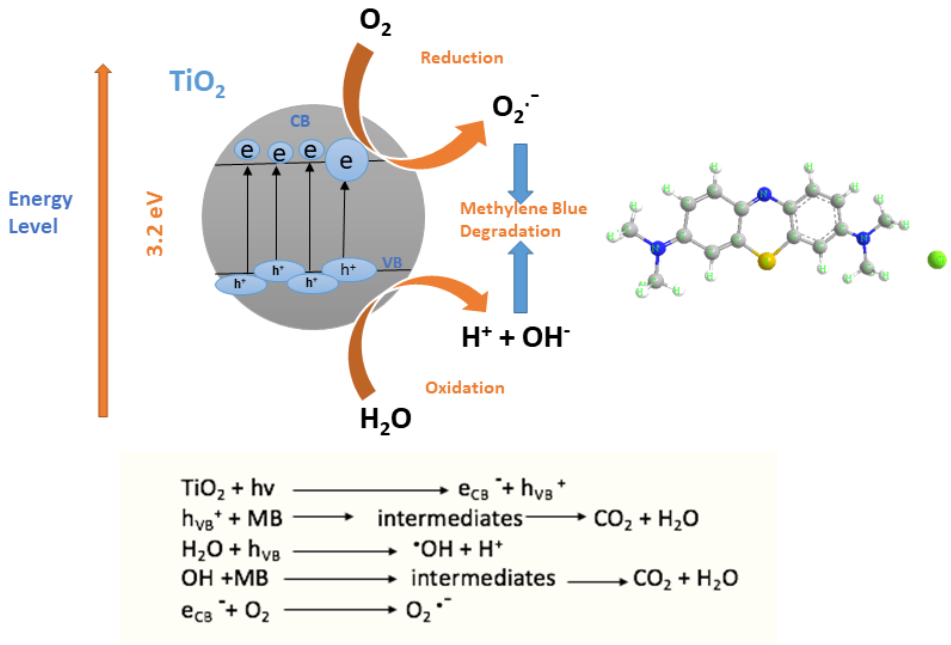

Figure 2.3 mechanism of MB photodegradation by TiO_2 semiconductor based on [53]

1.4.2. Bismuth Vanadate ($BiVO_4$)

$BiVO_4$ has been extensively employed as a highly responsive, visible-light driven, nontoxic, and photocatalyst with having narrow bandgap 2.4 eV. Various morphological has been well-defined for $BiVO_4$ such as sphere-like $BiVO_4$, flower-like $BiVO_4$, rod-like $BiVO_4$ and many others [54]. Photocatalytic degradation of organic compounds represents the area where $BiVO_4$

semiconductor is mostly applied [55]. In addition, $BiVO_4$ has been also used in the photoelectrocatalytic evolution of O_2 and H_2. But, the performance of $BiVO_4$ needs to be improved and that could be done using different methods [56]. There are three approaches; metal doping, metal deposition and coupling with other metal oxides [57]. It can be observed that the modified structures of $BiVO_4$ were more photocatalytically active more than pure structures. constructed composites exhibited well photocatalytic activity of certain catalysts by improving the electron-hole separation and reducing recombination process effectively [58]. For example, modified films ($InVO_4$-$BiVO_4$) were more photoactive in the degradation of MB than the pure films ($BiVO_4$) [59]. Another modified film based on a $BiVO_4$-TiO_2 composite was investigated for MB degradation in comparison with a pure $BiVO_4$ film. The modified films exhibited better degradation rates for MB as a result of enhanced electron transfer from CB of TiO_2 to CB of $BiVO_4$ and creation of favourable charge separation between them. Both $BiVO_4$-CuO powder [60] and $BiVO_4$ nanoparticles have been synthesised to examine their promising photocatalytic properties for MB photodegradation using visible light [61].

The mechanism for photocatalytic degradation of MB dye by $BiVO_4$ semiconductor is summarised in Figure 1.4 The electrons (e^-) are provided by photoexcitation of $BiVO_4$ may acquire enough energy 2.4 eV ($BiVO_4$ band gap) or more by absorb visible light to generate electron–hole pairs by excite the electron from VB and left a hole behind, which produce hydroxyl radicals(OH^-) by oxidizing MB molecules.

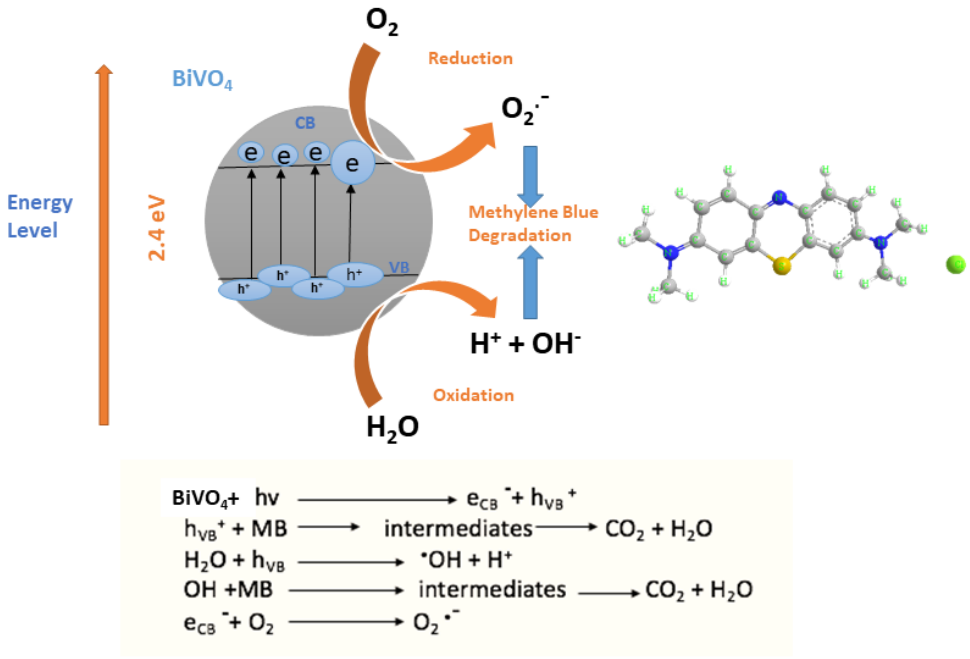

Figure 1.4 mechanism of MB photodegradation by $BiVO_4$ semiconductor based on [57]

1.5. Langmuir-Hinchelwood model

The Langmuir-Hinchelwood model, first described in 1921 by Irving Langmuir and developed later by Cyril Hinchelwood in 1926. It is widely applied to elucidate kinetics of heterogenous catalytic reactions which can be written as below:

$$r = -(dC / d_t) = (k_r KC / 1+KC')$$

r: rate of reaction based on time, C: concentration, t: time, k and K: oxidation rate constant and adsorption coefficient of the reactant, respectively. Also, this equation can be approximated to first order kinetics when KC << 1.

Integrating previous equation gives:

$\ln (C_t / C_0) + K (C_0 - C_t) = kKt$

C_0: initial concentration of MB (very diluted < 10^{-3} M), C_t: concentration at a time [62].

1.6. Factors Influencing Photocatalytic Dye Degradation

Photocatalytic degradation rates and the efficiency of photodegradation systems rely considerably on the operational parameters that drive the photodegradation process as mentioned in many correlated studies [35]. Some parameters have been discussed below to determine how rates of degradation can be increased or These parameters have been changed under solar simulator light with an AM1.5 filter an absolute air mass of 1.5, this filter simulates all the radiation which reach the earth, as it simulates the solar spectrum on the ground when solar zenith angle 48.19°s [63]

Dye concentration

The photocatalysis process can be influenced by the adsorption of dyes on the photocatalyst surface. In general, the photocatalysis reaction is affected only by the dye molecules adsorbed on the surface of a catalyst and not the dye in the bulk solution [35]. Increasing dye concentration has been shown to increase dye molecules adsorbed on the catalyst surface, thus, reducing the number of photons reaching the surface which could decrease the production of •OH radicals and the degradation rate of the dye as a consequence [35]. It can be concluded that, the photodegradation would be more effective with contaminants found in very low concentration [35]. The impact of dye concentration depends on two factors, the interaction between dye and

catalyst and the configuration of the reactor. If the reactor uses a film, which is on the side being illuminated, then the parasitic absorption of the dye is going to be quite small.

Temperature

The chemical reaction between catalyst surface and organic dye molecules can be either exothermic or endothermic. In the case of an endothermic reaction, adsorption phenomena can be greatly enhanced by increasing the temperature. This may be attributed to improving the kinetics energy of dye molecules which increasing their adsorption on the catalyst surface in return. Conversely, if increasing the temperature of the dye-adsorbent solution leads to reducing the capacity of adsorption, then, the reaction is exothermic [64]. The light source heating the reactor may have a much greater effect on the temperature which will then affect diffusion. Therefore, the effect of temperature needs further investigation.

pH value

The pH of the solution can alter the state of the dye removal reaction [65, 66].Changing the pH value can change the surface charge of the photocatalyst resulting in an alteration of the adsorbed species on the catalyst surface. Therefore, cationic dyes (positively charged) or anionic dyes (negatively charged) might be affected by changing the pH value of the reaction. Briefly, two things happen here, firstly changing pH can affect the degradation mechanism because it changes the concentration of photons or the concentration of hydroxy anions which were used to create radicals for the

degradation. Secondly, pH for the reaction can changes from pH for MB itself which around 3.5-4[64].

Adsorption is linked to isoelectric point of catalyst and degree of dissociation. Isoelectric point can be described as oxides surfaces or oxide-covered metals immersed in aqueous solutions with maintaining the hydroxyl groups unconjugated (forms an outermost layer of hydroxyl groups), so that, the oxide layer is called isoelectric point (PHpzc). At this point, the surface charge equals to zero, however, when the isoelectric point is greater than the PH, a positive charge will be needed to the surface.

Two kinds of reactions may occur in the outermost layer of surface hydroxyls defined as (i) proton association/ dissociation, (ii) cations or anions reaction to form the hydroxyl layer on the surface. This layer will then undertake association or dissociation based on PH value of the aqueous solution and the isoelectric point of the oxide film.

Catalyst concentration

Increasing the concentration of photocatalyst can benefit or impair dye degradation [67]**.** An increase in the number of the photons which can be adsorbed on the active sites of the photocatalyst will increase the number of •OH radicals and enhance removal efficiencies as a result [68]. some authors have observed that increasing catalyst concentration beyond a specific limit can decrease the percentage of dye degradation [69].

Light intensity

Using solar light irradiation to excite the photodegradation reaction can be more effective and reproducible on the reaction than the sunlight source

[70]. Light intensity has an effect on the reaction of dye degradation. At 0 to 20 mW / cm^2 (low light intensity), the degradation rate would be linearly increased by increasing the light intensity. Also, the rate of creating electron-hole pairs is greater than that of recombining them at this stage. Around 25 mW / cm^2 (intermediate light intensity), the degradation rate will be dependent on the square root of the applied light intensity[71]. When it comes to high light intensities, the rate of degradation would be independent and the creation and recombination of electron-hole pairs would take place significantly.

Reactor volume

Using different reactor volumes is expected to have an influence on the degradation rate. Increasing reactor volume, with an increase in the number of dye molecules, but without a change in the photocatalyst quantity, would lead to a decreased adsorption efficiency. Moreover, the degradation rate for the dye solution will increase with an increase in the reactor volume because of abatement of the light passing through the solution [72]. However, the reactor volume effect lacks uniformity in the literature. Therefore, in the current study, reactor volume has been considered as one of the factors which could have an effect on degradation rate of dyes.

Film size

The present study will focus on using photocatalyst films. Active sites on the photocatalyst surface which are facing the light source can dominate the rate of degradation [73]. Also, increasing the surface area leads to increased reaction rates by increasing the contact area between the liquid dye and the catalyst surface. Furthermore, the photocatalytic reaction can be improved as

more photons passing through the dye will be in contact with the catalyst's surface.

To illustrate; the catalytic performance from a 2 cm^2 film under 1 sun is not expected to be the same as 1 cm^2 film under 2 suns (with the same volume and at the same temperature). The different surface area of the films will give different catalytic results.

1.7. Beer-Lambert Law

The reactions produced by light absorbance give rise to a change or destruction of the molecules or the species absorbed which decreases the concentration of the latter. Subsequently, there is a shift in the light absorption rate, thus, leading to a reaction of these components.

The definition of the decrease in light (monochromatic light) intensity with an increase in the thickness and the concentration of the solution (can be solid or gas) through the transparent area is[74]

$A = \log_{10}(I_0 / I_i) = \varepsilon bc$

Where,

A = the absorbance of the aqueous solution at a specific wavelength

I_0 = Incident light intensity

I_i = Transmitted light intensity

ε = the absorbance of the molecular at the light intensity.

b = the path length (cm)

c = the concentration (moles/lit) There are some limitations to Beer-Lambert Law result in non-linear relation at specific conditions when:

- Reaching the equilibrium state by absorbed molecules having different structures.
- Formation of complex compounds between dissolved species (solute and solvent).
- Ground and excited electronic states are in thermal equilibrium.
- The reacted species are fluorescent or phosphorescent.

1.8. Figures of Merit

Different figures of merit have been established by the IUPAC (International union of pure and applied chemistry) for advanced oxidation processes (AOP systems). It provides a comparison when applying different AOP systems and also gives an idea about required costs. In terms of systems that include low concentration of contaminants, The lower electricity costs required to perform degradation of contaminants E_{EO} can be calculated as stated by Bolton et. al. [75]

$$E_{EO} = P / (V \times k_{app})$$

P: lamp power (kW) of a system being operated, V: volume (m^3), and k_{app}: pseudo first rate constant (h^{-1}), E_{EO}: lower electricity costs required to perform degradation of contaminants.

When using solar energy, illuminated collector area (A_{CO}) is needed. Then, figures of merit in the low concentration range can be established based on it as explained in the equation below:

$$A_{CO} = A_r E_S t / (V X K_{app})$$

A_r: illuminated collector area

E_S: is the solar irradiance [W m^{-2}]

In addition, the rate constants are then compared against the parameter being altered in each test to establish a relationship.

1.9. Aims and objectives

The chief aim is to compare results for different materials, collected in different conditions (including reactor volume, film size, temperature, initial concentration, thickness and light intensity) were all investigated and optimised by proposing figure of merit as an alternative of Langmuir Hinshelwood models. The results were based on two different materials; titanium dioxide (TiO_2-p25) and bismuth vanadate $BiVO_4$.

1.10. References

1. Maojun, W., et al., The Research on the Relationship between Industrial Development and Environmental Pollutant Emission. Energy Procedia, 2011. 5: p. 555-561.
2. Karaalp, H.S. and N.D. Yilmaz, Comparative advantage of textiles and clothing: Evidence for Bangladesh, China, Germany and Turkey. Fibres and Textiles in Eastern Europe, 2013. 97(1): p. 14-17.
3. Khan, S. and A. Malik, Environmental and Health Effects of Textile Industry Wastewater, in Environmental Deterioration and Human Health: Natural and anthropogenic determinants, A. Malik, E. Grohmann, and R. Akhtar, Editors. 2014, Springer Netherlands: Dordrecht. p. 55-71.
4. N W. Hines, Controlling Industrial Water Pollution: Color the Problem Green. (1968). 9 B.C.L. Rev. 553.
5. Kant, R., Textile dyeing industry an environmental hazard. Natural Science, 2012. Vol.04No.01: p. 5.
6. Ae, G., et al., Production, Characterization and Treatment of Textile Effluents: A Critical Review. Journal of Chemical Engineering & Process Technology, 2014.
7. Qasim, W. and A.V. Mane, Characterization and treatment of selected food industrial effluents by coagulation and adsorption techniques. Water Resources and Industry, 2013. 4: p. 1-12.
8. Vikramjit, S., R. Chhotu, and K. Ashok, - Physico-Chemical Characterization of Electroplating Industrial Effluents of.

9. Rani, S., et al., Removal of methylene blue and rhodamine B from water by zirconium oxide/graphene. Water Science, 2016. 30(1): p. 51-60.
10. Mills, A. and S. Le Hunte, An overview of semiconductor photocatalysis. Journal of Photochemistry and Photobiology A: Chemistry, 1997. 108(1): p. 1-35.
11. Ibhadon, A. and P. Fitzpatrick, Heterogeneous Photocatalysis: Recent Advances and Applications. Catalysts, 2013. 3(1): p. 189.
12. Hoffmann, M.R., et al., Environmental Applications of Semiconductor Photocatalysis. Chemical Reviews, 1995. 95(1): p. 69-96.
13. Photocatalysis by Nanostructured TiO2-based Semiconductors, in Handbook of Green Chemistry.
14. Tabaei, H.S.M., M. Kazemeini, and M. Fattahi, Preparation and characterization of visible light sensitive nano titanium dioxide photocatalyst. Scientia Iranica, 2012. 19(6): p. 1626-1631.
15. Bogdan, J., et al., Chances and limitations of nanosized titanium dioxide practical application in view of its physicochemical properties. Nanoscale Research Letters, 2015. 10(1): p. 57.
16. Xu, F.-L., et al., Persistent Organic Pollutants in Fresh Water Ecosystems. The Scientific World Journal, 2013. 2013: p. 2.
17. Gürses, A., et al., Dyes and Pigments: Their Structure and Properties, in Dyes and Pigments, A. Gürses, et al., Editors. 2016, Springer International Publishing: Cham. p. 13-29.
18. Bhatti, I.A., et al., Dyeing of UV irradiated cotton and polyester fabrics with multifunctional reactive and disperse dyes. Journal of Saudi Chemical Society, 2016. 20(2): p. 178-184.

19. Pereira, L. and M. Alves, Dyes—Environmental Impact and Remediation. 2012. 111-162.
20. Kuhad, R., et al., Developments in Microbial Methods for the Treatment of Dye Effluents. Vol. 56. 2004. 185-213.
21. Fujishima, A. and K. Honda, Electrochemical Photolysis of Water at a Semiconductor Electrode. Nature, 1972. 238: p. 37.
22. Gül, Ü.D., Treatment of dyeing wastewater including reactive dyes (Reactive Red RB, Reactive Black B, Remazol Blue) and methylene blue by fungal biomass. Water SA, 2013. 39: p. 593-598.
23. Sharifi Pajaie, S.H., S. Archin, and G. Asadpour, Optimization of Process Parameters by Response Surface Methodology for methylene blue Removal Using Cellulose Dusts. Vol. 4. 2018. 620.
24. Suteu, D. and T. Malutan, Industrial Cellolignin Wastes as Adsorbent for Removal of methylene blue Dye from Aqueous Solutions. BioResources; Vol 8, No 1 (2013), 2012.
25. P., F., R. A., and M.B. W., Methylthioninium chloride: pharmacology and clinical applications with special emphasis on nitric oxide mediated vasodilatory shock during cardiopulmonary bypass. Anaesthesia, 2005. 60(6): p. 575-587.
26. Miclescu, A., Cerebral protection in experimental cardiopulmonary resuscitation (with special reference to the effects of methylene blue). Vol. 54. 2009.
27. Rafatullah, M., et al., Adsorption of methylene blue on low-cost adsorbents: A review. Journal of Hazardous Materials, 2010. 177(1): p. 70-80.

28. Abu Ghalwa, N.M. and F.R. Zaggout, Electrodegradation of methylene blue Dye in Water and Wastewater using Lead Oxide/Titanium Modified Electrode. Journal of Environmental Science and Health, Part A, 2006. 41(10): p. 2271-2282.

29. Herrmann, Jean-Marie, Heterogeneous photocatalysis: Fundamentals and applications to the removal of various types of aqueous pollutants. Vol. 53. 1999. 115-129.

30. Houas, A., et al., Photocatalytic degradation pathway of methylene blue in water. Applied Catalysis B: Environmental, 2001. 31(2): p. 145-157.

31. Forgacs, E., T. Cserháti, and G. Oros, Removal of synthetic dyes from wastewaters: a review. Environment International, 2004. 30(7): p. 953-971.

32. Orecki, A., et al., Surface water treatment by the nanofiltration method. Desalination, 2004. 162: p. 47-54.

33. Strathmann, H., Electrodialysis and Its Application in the Chemical Process Industry. Separation and Purification Methods, 1985. 14(1): p. 41-66.

34. Mehta, D.J. and A.V. Rao, Reverse-Osmosis Research in India: Scope and Potentialities, in Synthetic Membranes:. 1981, AMERICAN CHEMICAL SOCIETY. p. 293-303.

35. Kumar, A., A Review on the Factors Affecting the Photocatalytic Degradation of Hazardous Materials. Vol. 1. 2017.

36. Liang, R., et al., Fundamentals on Adsorption, Membrane Filtration, and Advanced Oxidation Processes for Water Treatment. Vol. 22. 2014. 1-45.

37. Salleh, A., et al., Cationic and Anionic Dye Adsorption by Agricultural Solid Wastes: A Comprehensive Review. Vol. 280. 2011. 1-13.

38. Jafari, T., et al., Photocatalytic Water Splitting—The Untamed Dream: A Review of Recent Advances. Molecules, 2016. 21(7): p. 900.

39. Li, R., et al., Visible-Light Induced High-Yielding Benzyl Alcohol-to-Benzaldehyde Transformation over Mesoporous Crystalline TiO2: A Self-Adjustable Photo-oxidation System with Controllable Hole-Generation. The Journal of Physical Chemistry C, 2011. 115(47): p. 23408.

40. Goudon, T., V. Miljanović, and C. Schmeiser, *On the Shockley–Read–Hall Model: Generation-Recombination in Semiconductors.* SIAM Journal on Applied Mathematics, 2007. **67**(4): p. 1183-1201.

41. Hernández-Alonso, M.D., et al., Development of alternative photocatalysts to TiO2: Challenges and opportunities. Energy & Environmental Science, 2009. 2(12): p. 1231-1257.

42. Bickley, R.I., Photo-induced reactivity at oxide surfaces, in Chemical Physics of Solids and Their Surfaces: Volume 7, M.W. Roberts and J.M. Thomas, Editors. 1978, The Royal Society of Chemistry. p. 118-156.

43. Bedja, I., S. Hotchandani, and P. Kamat, Photoelectrochemistry of quantized WO3 colloids. Electron storage, electrochromic, and photoelectrochromic effects. Vol. 97. 1993.

44. Ishchenko, O.M., et al., TiO2- and ZnO-Based Materials for Photocatalysis: Material Properties, Device Architecture and Emerging Concepts, in Semiconductor Photocatalysis - Materials, Mechanisms and Applications. 2016.

45. Yunus, I.S., et al., Nanotechnologies in water and air pollution treatment. Environmental Technology Reviews, 2012. 1(1): p. 136-148.

46. Etacheri, V., et al., Visible-light activation of TiO2 photocatalysts: Advances in theory and experiments. Journal of Photochemistry and Photobiology C: Photochemistry Reviews, 2015. 25: p. 1-29.

47. Pawar, M., et al., A Brief Overview of TiO2 Photocatalyst for Organic Dye Remediation: Case Study of Reaction Mechanisms Involved in Ce-TiO2 Photocatalysts System. Journal of Nanomaterials, 2018. 2018: p. 13.

49. Nakata, K. and A. Fujishima, TiO2 photocatalysis: Design and applications. Journal of Photochemistry and Photobiology C: Photochemistry Reviews, 2012. 13(3): p. 169-189.

50. Nawawi, W., et al., The Preparation and Characterization of Immobilized TiO2/PEG by Using DSAT as a Support Binder. Applied Sciences, 2017. 7(1): p. 24.

51. Akpan, U.G. and B.H. Hameed, Parameters affecting the photocatalytic degradation of dyes using TiO2-based photocatalysts: A review. Journal of Hazardous Materials, 2009. 170(2): p. 520-529.

52. Xu, C., G.P. Rangaiah, and X.S. Zhao, Photocatalytic Degradation of methylene blue by Titanium Dioxide: Experimental and Modeling Study. Industrial & Engineering Chemistry Research, 2014. 53(38): p. 14641-14649.

53. Chin, S., et al., Photocatalytic degradation of methylene blue with TiO2 nanoparticles prepared by a thermal decomposition process. Powder Technology, 2010. 201(2): p. 171-176.

54. Kunfeng Zhang, J.D., Yuxi Liu, Shaohua Xie and Hongxing Dai. , Photocatalytic Removal of Organics over BiVO4-Based Photocatalysts, Semiconductor Photocatalysis - Materials, Mechanisms and Applications. , Wenbin Cao, IntechOpen, 2016.

55. Pingmuang, K., et al., Composite Photocatalysts Containing BiVO4 for Degradation of Cationic Dyes. Scientific Reports, 2017. 7(1): p. 8929.

56. Liu, E.Y., et al., Understanding Photocharging Effects on Bismuth Vanadate. ACS Applied Materials & Interfaces, 2017. 9(27): p. 22083-22087.

57. Kalanoor, B.S., H. Seo, and S.S. Kalanur, Recent developments in photoelectrochemical water-splitting using WO3/BiVO4 heterojunction photoanode: A review. Materials Science for Energy Technologies, 2018. 1(1): p. 49-62.

58. Zhang, Q., et al., Constructing the magnetic bifunctional graphene/titania nanosheet-based composite photocatalysts for enhanced visible-light photodegradation of MB and electrochemical ORR from polluted water. Scientific Reports, 2017. 7(1): p. 12296.

59. Lamdab, U., et al., InVO4–BiVO4 composite films with enhanced visible light performance for photodegradation of methylene blue . Catalysis Today, 2016. 278: p. 291-302.

60. Abdullah, A., Degradation of methylene blue dye by CuO-BiVO4 photocatalysts under visible light irradiation. Vol. 20. 2016. 1338-1345.

61. Sivakumar, V., et al., BiVO4 nanoparticles: Preparation, characterization and photocatalytic activity. Cogent Chemistry, 2015. 1(1): p. 1074647.

62. Houas, A., et al., Photocatalytic degradation pathway of methylene blue in water. Applied Catalysis B: Environmental, 2001. 31(2): p. 145-157.

63. Yunus, W.M. and A.B. Rahman, Refractive index of solutions at high concentrations. Appl Opt, 1988. **27**(16): p. 3341-3

64. Yagub, M.T.A., Removal of methylene blue contaminant by natural and modified low cost agricultural by-product. 2013.

65. Qi, J., et al., Simultaneous removal of methylene blue and copper(II) ions by photoelectron catalytic oxidation using stannic oxide modified iron(III) oxide composite electrodes. J Hazard Mater, 2015. 293: p. 105-11.

66. Rahman, M., S. M Ruhul Amin, and A. M Shafiqul, Removal of methylene blue from Waste Water Using Activated Carbon Prepared from Rice Husk. Vol. 60. 2012.

67. Wei, T.Y., Heterogeneous photocatalytic oxidation of phenol with titanium dioxide powders. Industrial & engineering chemistry research. 30(6): p. 1293-1300.

68. Herrmann, J.M., Heterogeneous photocatalysis: an emerging discipline involving multiphase systems. Catalysis Today, 1995. 24(1): p. 157-164.

69. Kamble, S.P., S.B. Sawant, and V.G. Pangarkar, Batch and Continuous Photocatalytic Degradation of Benzenesulfonic Acid Using Concentrated Solar Radiation. Industrial & Engineering Chemistry Research, 2003. 42(26): p. 6705-6713.

70. Neppolian, B., et al., Solar/UV-induced photocatalytic degradation of three commercial textile dyes. J Hazard Mater, 2002. 89(2-3): p. 303-17.

71. Ollis, D.F., E. Pelizzetti, and N. Serpone, Photocatalyzed destruction of water contaminants. Environmental Science & Technology, 1991. 25(9): p. 1522-1529.

72. Iovino, P., et al., Degradation of Ibuprofen in Aqueous Solution with UV Light: the Effect of Reactor Volume and pH. Water, Air, & Soil Pollution, 2016. 227(6): p. 194.

73. Zhu, J., et al., Hydrothermal doping method for preparation of Cr3+-TiO2 photocatalysts with concentration gradient distribution of Cr3+. Applied Catalysis B: Environmental, 2006. 62(3): p. 329-335.

74. Dariani, R.S., et al., Photocatalytic reaction and degradation of methylene blue on TiO2 nano-sized particles. Optik - International Journal for Light and Electron Optics, 2016. 127(18): p. 7143-7154.

75. Bolton, J., et al., Figures-of-Merit for the Technical Development and Application of Advanced Oxidation Technologies for both Electric- and Solar-Driven Systems. Pure and Applied Chemistry, 2001. **73**: p. 617-637.

CHAPTER 2

EXPERIMENTAL METHODS

This chapter will focus on chemicals and reagents, equipment and techniques and gives details on all experimental procedures used in this research. All equipment (Agilent 8453 UV-visible Spectroscopy, The Veeco Dektak 150 profilometer, Screen-Printing technology, the laser cutter, the refrigerated Circulated bath system, LCS-100 solar simulator) were ~~used was~~ supplied by the University of Wollongong, Intelligent Polymer Research Institute (IPRI).

2.1 Preparation Stages of Photocatalyst Films

The synthesis of photocatalyst films was carried out over two stages. Paste preparation was followed by screen-printing of the films.

2.1.1 Photocatalyst Paste Preparation

The photocatalytic pastes were prepared from titanium dioxide (TiO_2) particles supplied by Merck), and bismuth vanadate ($BiVO_4$) was obtained from Kanlaya Pingmuang). The $BiVO_4$ particle synthesis differed significantly by included microwave irradiation. The details are given below.

2.1.1.1. TiO_2 (P25) Paste Preparation

One gram of TiO2 (Merck, P25) nanoparticle powder was blended with 0.2 mL of acetic acid ($C_2H_4O_2 \geq 99.0\%$ purity ,was obtained from Ajax Finechem) for 5 min followed by the addition of 1 mL of deionised water (DI) and grinding in a mortar and pestle for about 10 min. Ethanol (purity

≤100%,was supplied from Sigma-Aldrich) was added 25 mL (on several times) and thoroughly blended. Separately, 0.5 g of ethyl cellulose nanoparticle powder ($C_{20}H_{38}O_{11}$, Sigma-Aldrich product), was mixed with 4.5 g of ethanol (about 3 mL) and 6.5 g of anhydrous terpineol ($C_{10}H_{18}O$, purity ≤100%, puchased from Merck) which was stirred until a homogeneous mixture was obtained. The two mixtures were combined, sonicated and stirred for 1 hour, respectively. The rotary evaporator was used to evaporate the ethanol from the mixture [30 min at 100 mbar and 2 hours at 60 mbar].

2.1.1.2. $BiVO_4$ Paste Preparation

$BiVO_4$ screen printing paste and the particles was already produced using nanopartical synthesis by Kanlaya Pingmuang [1].

2.1.2. Screen-Printing

A plain sheet of glass was used as a substrate for the photocatalytic films. This sheet was sequentially cleaned prior to use, first by distilled water, then by sonication for 10-15 minutes in a container of soapy water, then sonication in acetone (C_3H_6O >98 % purity, was obtained from Chem-Supply) and finally ethanol for 1 hour each.The screen was made from a woven mesh of nylon or polyester and tensioned from the sides by a metal frame.

The paste was placed on the screen (which had been washed with ethanol then Squeegeed). The glass was positioned under the screen. The paste was pushed through the screen by moving the squeegee with downward pressure so the paste would form the required patterns from the screen. Figure 2.1. illustrates the steps of Screen-Printing technology.

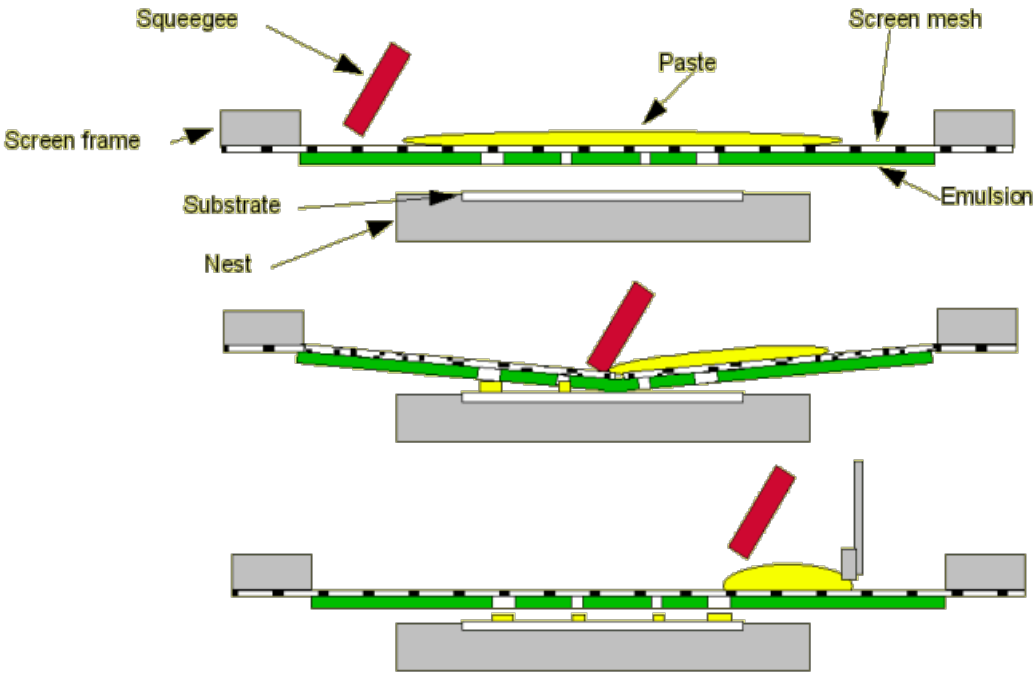

Figure 2.1 Schematic Illustration of Screen-Printing technology. Based on [2].

Printing was followed by drying to remove the solvent from the printed films by heating the films up to 120 °C for 15 min (Figure 2.2. B). To increase the number of layers (for thicker films), the previous procedure was repeated depending on the number of layers required. Once the desired film thickness was attained, a hot plate was used for annealing films at 450 °C to eliminate the nonvolatile organic components (binder) in the paste (Figure 2.2.C).

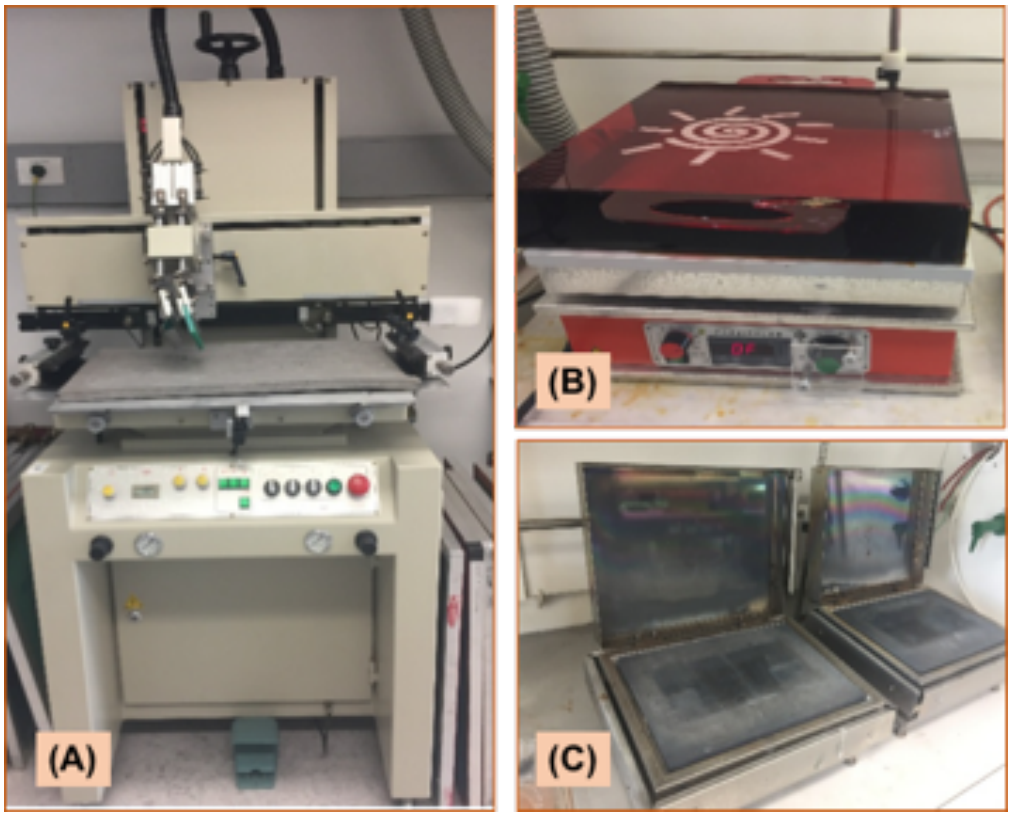

Figure 2.2 Images of (A) Screen-printer equipment, provided by Kang Yuan Industrial CO.LTD, type: KY-500FH, (B) and (C) Hot Plates

The screen-printed films of $BiVO_4$ and TiO_2, were created in rectangular shapes and printed on plain glass substrates with different dimensions as explained in Figure 2.3. Samples, or films, have been prepared in different layers and plates. Each plate has 8 printed films designed in similar and different dimensions. Moreover, four thickness of each photocatalyst were printed, the dimensions were as follows: 2 x 1 cm, 2 x 2 cm, 2 x 3 cm and 2 x 4 cm.

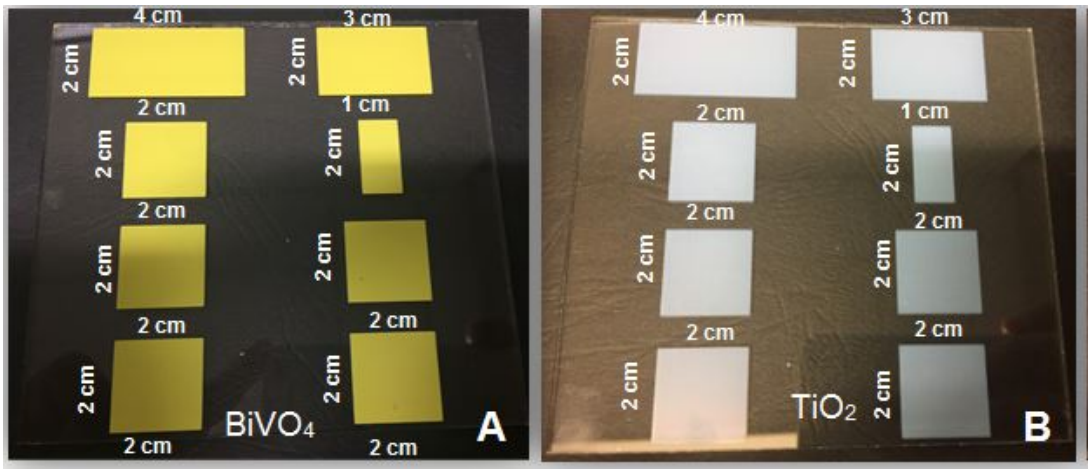

Figure 2.3 Images of screen-printed films on plain glass made of: (A) $BiVO_4$, (B) TiO_2

2.1.3. Preparation of MB Dye Solution

A concentration of 5 mmolar stock solution of MB dye was prepared by dissolving (0.799) g of MB powder ($C_{16}H_{18}ClN_3S \geq 82\%$ purity) purchased from Sigma Aldrich in (500) ml reverse osmosis water, then diluted to (2 mM,1 mM, 500 µM, 200 µM, 100 µM, 45 µM, 20 µM, 10 µM), 45 µM was used in most of the experiments in this research.

2.2. Reactors

2.2.1. Designing and Cutting Reactor Sheets using Laser Cutter

Custom reactors were built to test the effect of reactor volume and temperature by using a laser cutter/engraver (Versa laser ,10.6 µm and ~~defcult~~ default cutting settings to cut 3mm PMMA (extruded). This allowed the creation of reactors which were identical in all aspects except for volume.

The aim was to verify the relationship between degradation rate and reactor volume, film, illumination and temperature. CorelDRAW Graphic

Design 2016 was used to draw the shape and specify dimensions which were then constructed into a reactor (Figure 2.4 A,B). Table 2.1 shows the dimensions and thickness of the reactors . The sheets were made of PMMA, also known as acrylic or acrylic glass with a thickness of 0.3 cm. The height and the width of the reactor were kept constant (4.5 cm and 2.4 cm, respectively) for all designed reactors while the length only was changed depending on reactor volumes required. Also, a spin bar (0.45 cm diameter) was positioned in the bottom centre of the reactor (to avoid scratching of the photocatalytic film). The thickness of glass substrates used to screen-print the photocatalyst films was taken into consideration. Below is the equation used for calculating the volume of a reactor:

Volume of the reactor (V) = length (L) * width (W) * height (H).

volume of each reactor (ml)	**height (cm)**	**width (cm)**	**length (cm)**
5	**4.5**	**2.4**	**0.46**
10	**4.5**	**2.4**	**0.925**
20	**4.5**	**2.4**	**1.85**
50	**4.5**	**2.4**	**4.62**
100	**4.5**	**2.4**	**9.25**

Table 2. 1 Internal dimensions and thickness used for reactor fabrication

(0.2 cm allowance in the length of the reactor was made for all calculations to account for the thickness of the glass substrates)

The sheets were carefully cut using the Laser cutter and assembled using chloroform ($CHCl_3$, 99.8 % purity, was purchased from Merck) to give the final shape of the reactor as shown in figure 2.4 A.

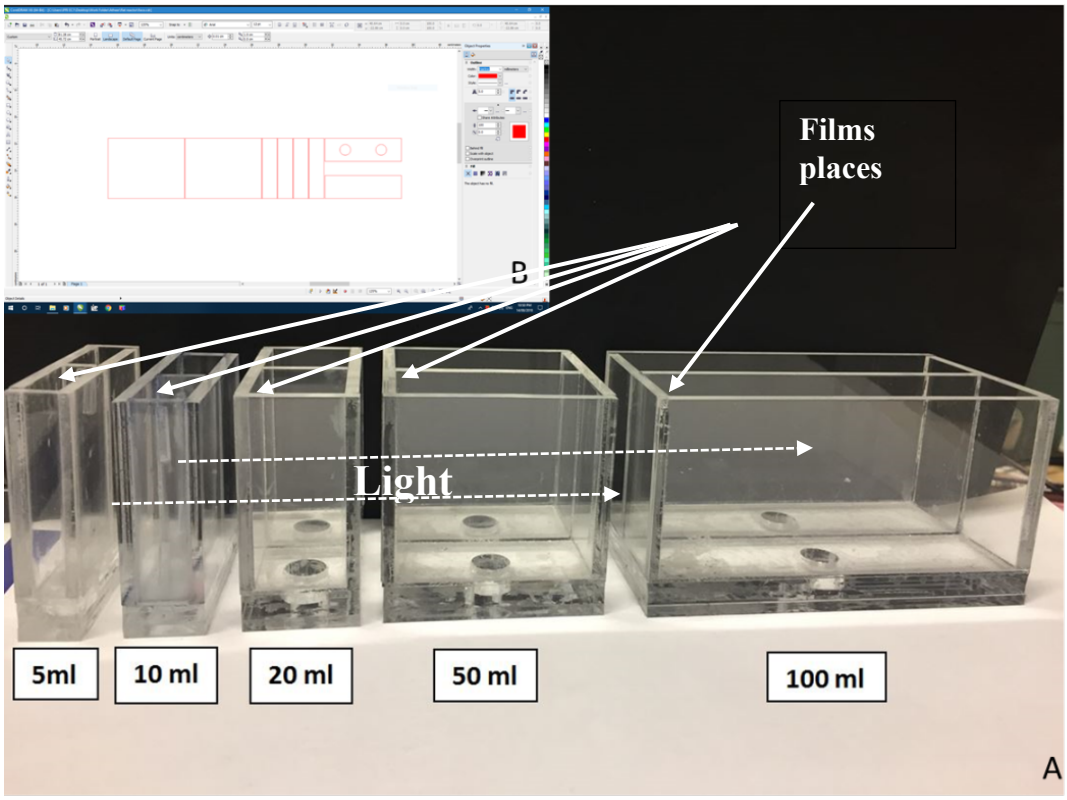

Figure 2.4.A image of five reactors (5 ml, 10 ml, 20 ml, 50 ml, 100 ml), B: Screenshot of CorelDRAW file showing how the sheets are assembled into the reactor form.

2.2.2. Designing a Reactor with a cooling and heating system

To study dye degradation rate at lower temperatures (from 1 – 5 ˚C) a modified reactor. An additional panel which contained a cooling circuit with a

recirculating liquid (ethylene glycol mixture, $C_2H_6O_2$,99.5% (w/v), was purchased from Fluka) was attached. The wall between the cooling circuit and the reactor was thin (0.5 mm) to maximise heat transfer. The bath system controlled the temperature between (-5°C to +80°C). Ethylene glycol in the bath tank was cooled to the required temperature then circulated between the bath and the reactor in order to cool the liquid in the reactor.

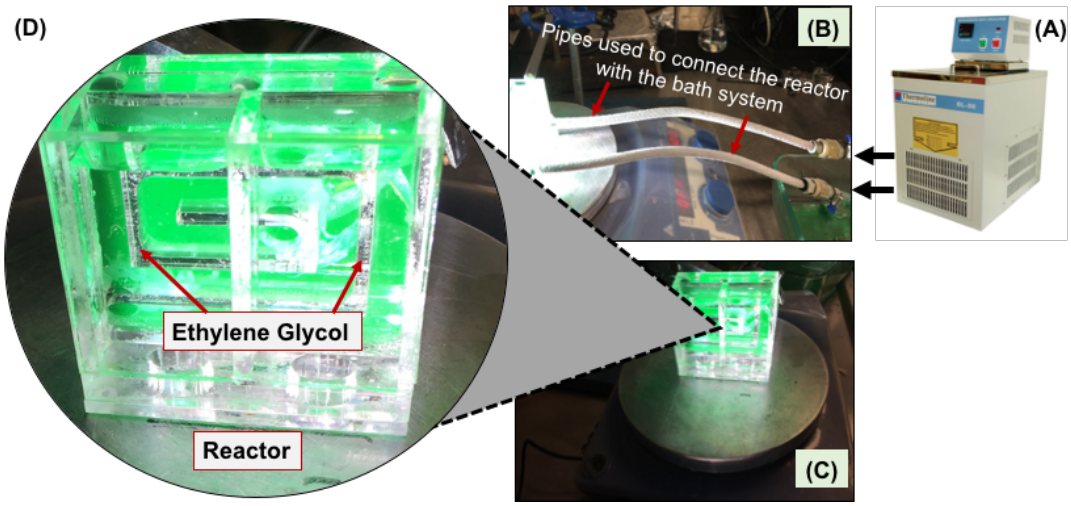

Figure 2.5 (A) Photograph of the refrigerated Circulated bath system (based on the manual book) [3]. (B, C, & D) images of the reactor with the designed cooling system

2.3. Photocatalysis Setup

Screen-printed photocatalyst films were tested for the degradation of MB dye solution using simulated solar illumination equipment (AM1.5G, 1 sun equivalent, 100 mW cm^{-2}).

The MB stock solution (5 mM) was prepared then diluted to 45 µM of dye which was used to fill the reactor in the presence of the film of photocatalyst

(TiO_2, $BiVO_4$). This was allowed to reach an adsorption/desorption equilibrium overnight.

The reactor was exposed to simulated sunlight (AM1.5) using the LCS-100 solar simulator while being stirred (Figure 2.6). At 15 min intervals, a ~1 mL sample was collected, its absorbance was measured by an Agilent 8453 UV-vis spectroscopy system, then returned to the reactor. The total exposure time was 180 minutes.

Furthermore, the light intensity was varied by change the distance between the light source (the LCS-100 solar simulator) and the reactor.

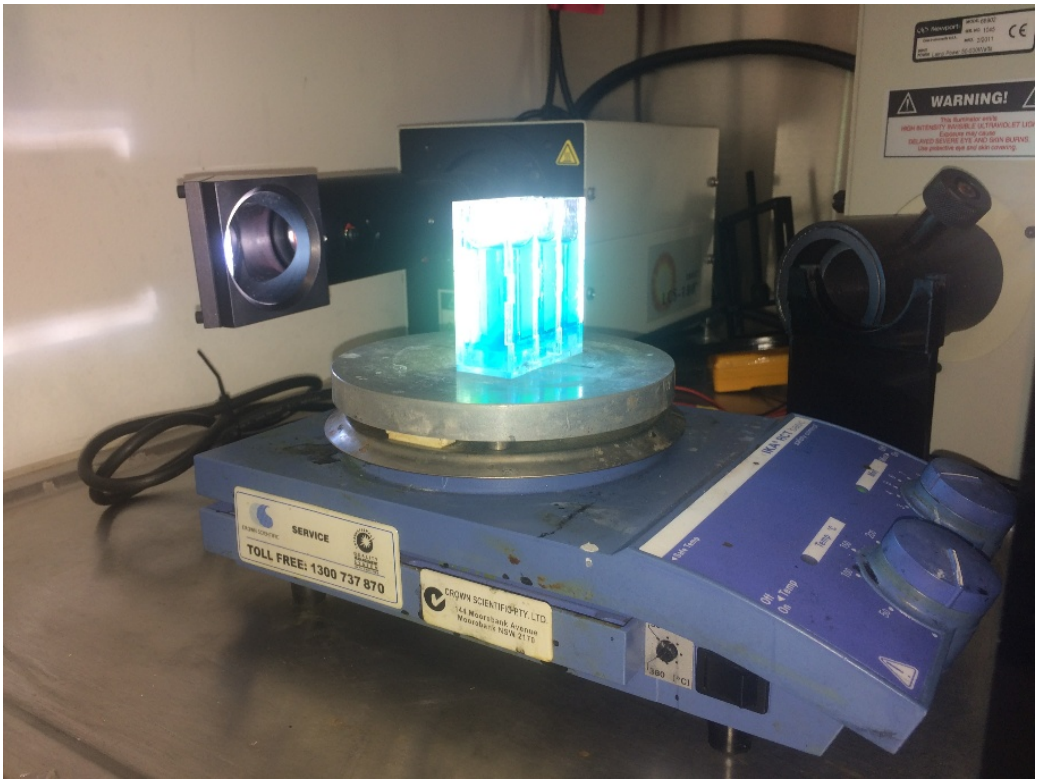

Figure 2.6 Image of LCS-100 solar simulator

2.4. Physical Characterization Methods

2.4.1. Agilent 8453 UV-visible Spectrophotometry

Spectrophotometry is invaluable for the study of photocatalytic degradation of dyes. Here, the Agilent 8453 UV-vis-spectrophotometer was used to obtain transmittance spectra of samples taken during testing of films to determine their photodegradation performance towards MB. The Agilent 8453 has a wavelength range of 190 – 1100 nm (with 1 nm resolution), and utilises Photodiode Array detectors and both Deuterium and Tungsten illumination sources [4].

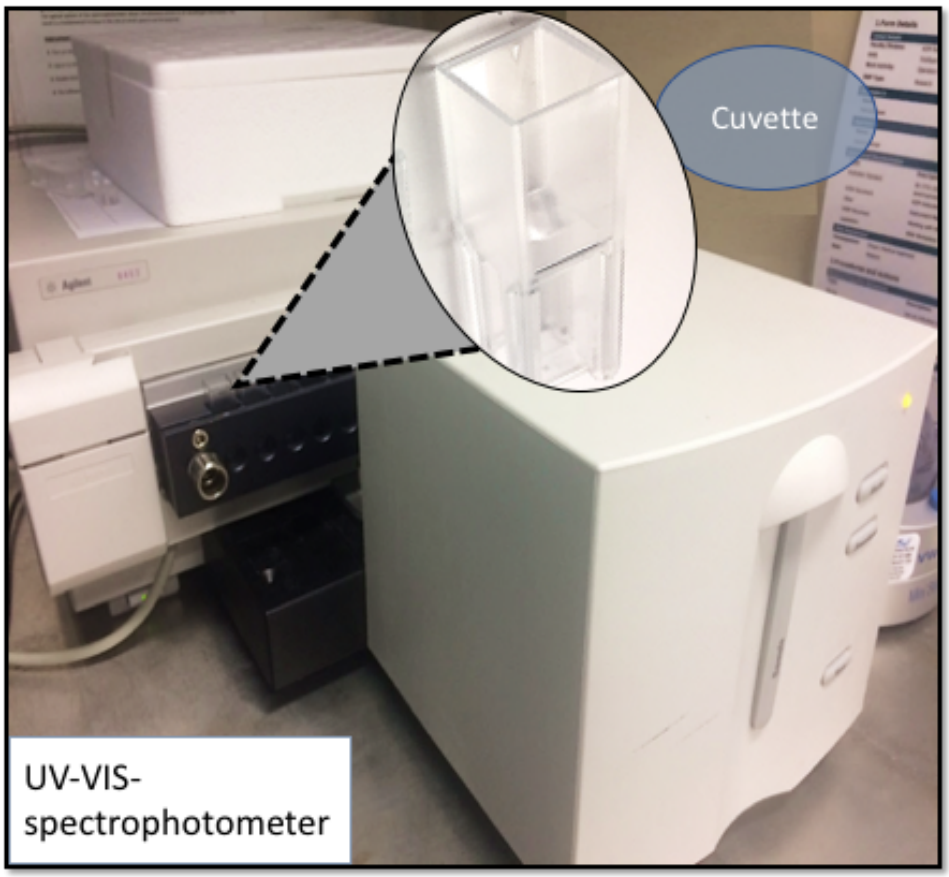

Figure 2.7 Image of Agilent 8453 UV-visible spectrophotometer

2.4.2. Profilometer – Veeco Dektak 150

The Veeco Dektak 150 profilometer employs the Low-Inertia Sensor 3 (LIS 3) instead of using a mechanical probe to investigate material superficies by moving the Sensor over the material surface to investigate the height of the

material [5]. This instrument provides 2D measurements with a 1-15 mg stylus strength. The stylus transmits information about the changing height of the surface detected as a vertical change which is deciphered and transferred as an electrical signal to the signal reception.

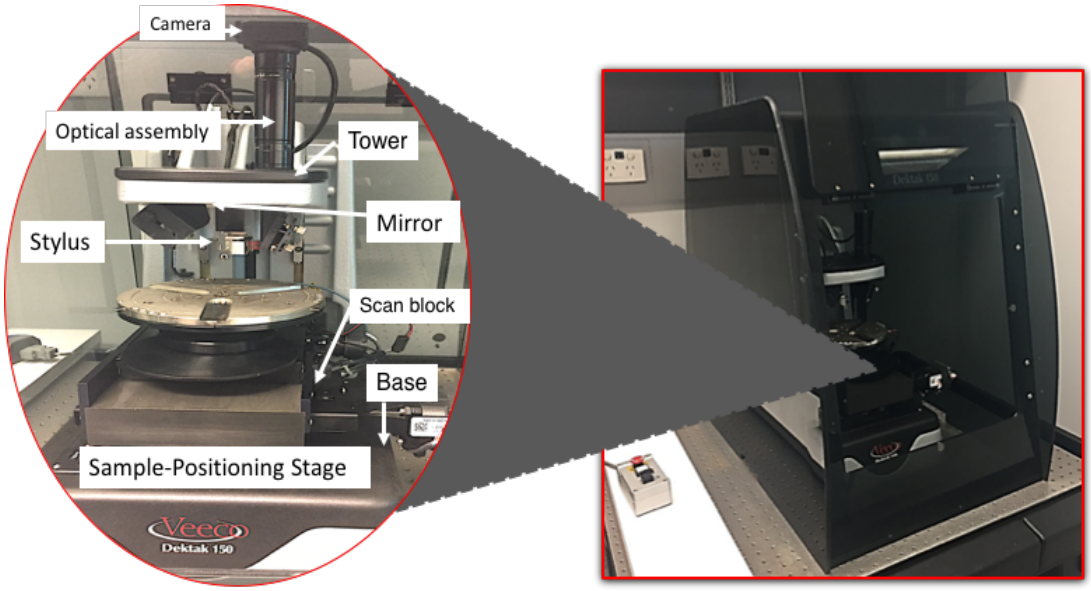

Figure 2.8 Image of Profilometer -Dektak 150

2.5. References

1. Pingmuang, K., et al., Photocatalytic Mineralization of Organic Acids over Visible-Light-Driven Au/BiVO4 Photocatalyst. International Journal of Photoenergy, 2013. 2013: p. 7.
2. Hobby, A., SCREEN PRINTING FOR THE INDUSTRIAL USER. 1997, Gwent Group: United Kingdom.
3. Scientific, T., refrigerated circulated bath. 2019, Thermoline Scientific : Australia.
4. Czegan, D.A.C. and D.K. Hoover, UV–Visible Spectrometers: Versatile Instruments across the Chemistry Curriculum. Journal of Chemical Education, 2012. **89**(3): p. 304-309.
5. Seitavuopio, P., The roughness and imaging characterisation of different pharmaceutical surfaces. 2018.

CHAPTER 3

"EFFECT OF PHYSICAL PARAMETERS ON PHOTOCATALYTIC DEGRADATION OF MB IN THE PRESENCE OF TiO_2 AND $BiVO_4$ PHOTOCATALYST FILMS"

3.1. Introduction

Most of the published studies regarding the effect of operation factors on photocatalytic degradation of MB were focusing on: (1) improving the efficiency of degradation process, and (2) creating kinetic models based on the concentration of the targeted dye. Notably, experimental setup being used and employed conditions are important for the validity of the kinetic expressions.

This study focuses on the photodegradation of MB as a model dye in the presence of commonly used catalysts TiO_2 and $BiVO_4$ [1, 2] as screen-printed films. Moreover, the effect of operating factors such as catalyst loading, initial dye concentration, reaction temperature, reactor volume, and films thickness and size were all investigated. The testing approach was based on varying one of the factors and keeping the others constant for every test. For example, investigating the effect of changing reactor volumes (from 5 up to 50) ml while maintaining reaction temperature, initial concentration, films size and thickness, and catalyst loading the same. The effect of another factor such as varying reaction temperature while keeping the rest of the factor's constant was investigated as well until all of them were completed. Notably, Figures of Merit regard low concentration of a contaminant has been chosen here to compare the above factors based on different materials and evaluate if they behave in the same way. Furthermore, the materials did not need to be characterised as we are not introducing a newly synthesised material. The TiO_2 and $BiVO_4$ were taken, then, excited and measured under controlled conditions to find a better way to compare different materials.

3.2. Evaluation of Photocatalytic Activity:

Photocatalytic performance of prepared films (TiO_2, $BiVO_4$) was tested using Solar Stimulator (LCS-100TM ORIEL®) to investigate photocatalytic degradation of MB dye. The films were inserted in 5 ml ,10 ml, 50 ml, 100 ml reactors separately (each reactor containing 45 μM of MB) and placed in the dark for 2:30 h to reach the adsorption-desorption equilibrium state and test them by UV-vis spectrophotometer later. The same MB samples were then placed on a stirrer under simulated solar illumination (with an AM1.5 filter) from the side and repeated every 15 min up to 3 hours. The testing procedure included measure the absorbance of MB solution in a PMMA (disposable) cuvette, from 190 – 1060 nm, using Agilent 8453 UV-visible Photospectrometry. The concentration was calculated based on the absorbance of the peak of 664nm, assuming a linear relationship (verified below). The rate constant was measured using the following equation:

% remaining of MB= $((C_0-C) / C_0) \times 100$, where C_0 the concentration of MB at t=0. C is the remaining concentration of MB in the solution.

3.3. Results and Discussion

3.3.1. Adsorption of MB dye on the reactor walls (in the absence of photocatalyst)

MB dye (45μM) in aqueous solution was transfer to (10 ml) reactor volume for a period of time then take it off the reactor, the results show that the walls of the reactor does not colored with the dye color, which means that a minimum of dye adsorbed on the reactor.

3.3.2. Studying the effect of initial concentration on photodegradation rate of MB

Dye concentration factor was tested in this study to find out potential effect can be made on calibration curve when varied. In this experiment, series of MB concentrations 10, 20, 50, 100, 200, 500, 1000, 2000 and 5000 μM were prepared and transferred into UV cuvette for further recordings. Herein, UV cuvette itself were designed in different volumes listed as 1, 0.83, 0.3, 0.14, and 0.04 cm. Each concentration of MB was tested in varied cuvette volumes as explained in the table (3.1). The aim of this experiment is to obtain and compare the absorbance and extinction coefficient of examined MB concentrations using different pathlengths to evaluate the Beer-Lambert with this system. For these reasons, four different cuvettes were made with various pathlengths figure (3.1) with considering the dimensions around 45 mm high and 4 mm width to fit in the UV-vis instrument.

It's worth mentioning that, when a solution concentration is high, its molecules can have aggregation. As the absorption of UV-visible based on electronic transferring process, testing high concentration solutions may shift the absorption of targeted molecules. Not only this, the refractive index (η) of highly concentrated solutions can be changed and obtain altered absorbance value[4]

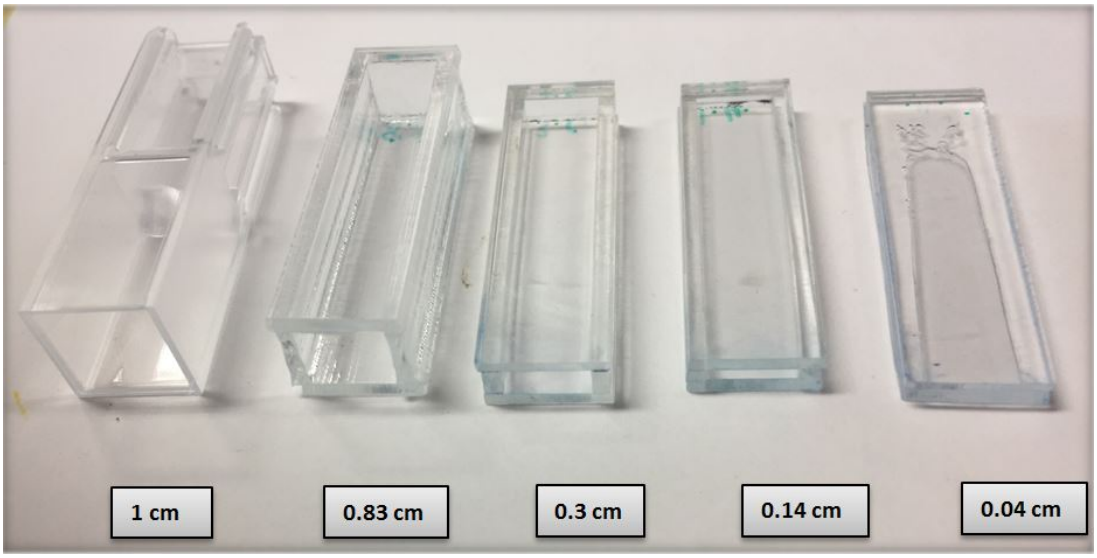

Figure 3.1 image of comparing the four cuvettes made in this research and the original (the standard 1 cm) cuvette

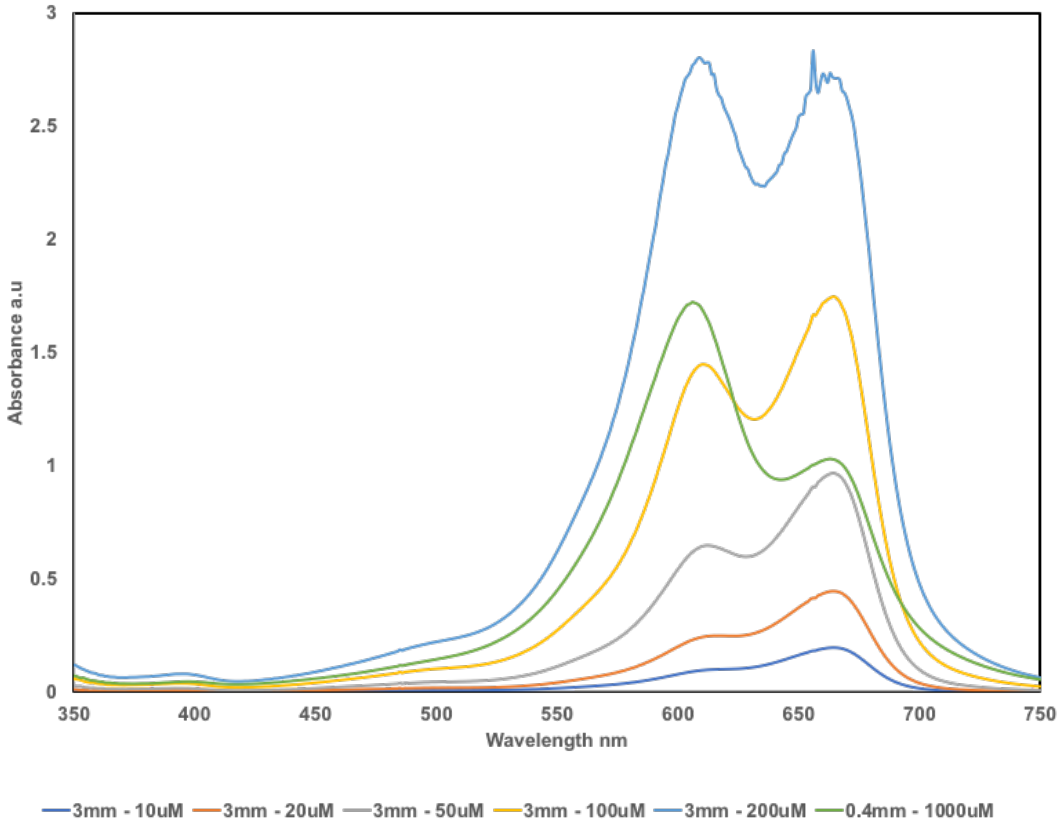

Figure 3.2 UV-vis spectra showing the aggregation of high concentration for different concentrations of MB dye using different

pathlength, 3mm - 10 µM,3mm – 20 µM, 3mm – 50 µM, 3mm – 100 µM, 3mm – 200 µ, 0.4mm - 1000µM.

The concentrations of 10 µM, 20 µM, and 50 µM were examined by (1 cm, 0.83 cm, 0.3 cm, and 0.14 cm) cuvettes and 50 µM was further tested by 0.04 cm cuvette. It can be noted in figure (3.3) that, the extinction co-efficient shows an approximately linear relationship with increasing the initial concentration from 10 µM- 50 µM which means the relation between concentration and absorbance is linear. For concentrations higher than 50 µM, such as 100 µM up to 1000 µM, the extinction co-efficient showed a continuous drop. This behaviour has been explained as high concentrations of MB might display the aggregation problem as well as surface dimerization phenomenon [5].

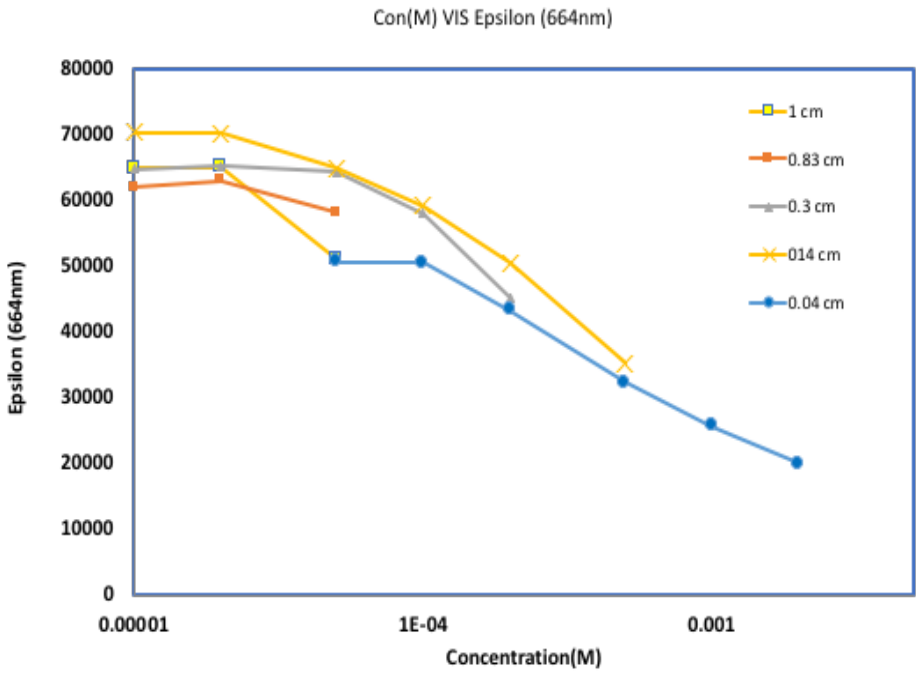

Figure 3.3 the relationship between MB dye concentrations (M) vs extinction co-efficient at 664 nm on 25 °C, 100 mW cm^{-2}

Conc. µM	Pathlength (cm)
10 µM	1, 0.3, 0.14, 0.83
20 µM	1, 0.3, 0.14, 0.83
50 µM	1, 0.3, 0.14, 0.83, 0.04
100 µM	0.3, 0.14, 0.04
200 µM	0.3, 0.14, 0.04
500 µM	0.14, 0.04
1000 µM	0.04
2000 µM	0.04
5000 µM	0.04

Table 3. 1 Tested concentrations of MB at varied cuvette volumes

For the dilute solutions, the peak absorbance at 660 is quite strong, this one at 620 nm is weaker, for the high concentration solution it clearly shows that the ratio between these peaks is much less, for the very high concentration the spectra significantly change.

The electronic states of molecules change as they assemble to form aggregates[6] because the interaction between these molecules, high dye concentration could easily result in the formation of aggregates due to dye self-interaction and reaching the solubility limit, some dyes are naturally more attractive to each other[6].

3.3.3. Typical set up

The standard set of conditions which were used in the experiments are 2 cm X 2 cm film size, 10 ml reactor volume, 25°C reaction temperature, 100 mw cm^{-2} and one-layer film thickness., 45μM MB dye. To control system so it's can be varying each parameter systematically. One condition of these five was varied every time to keep the other conditions constant.

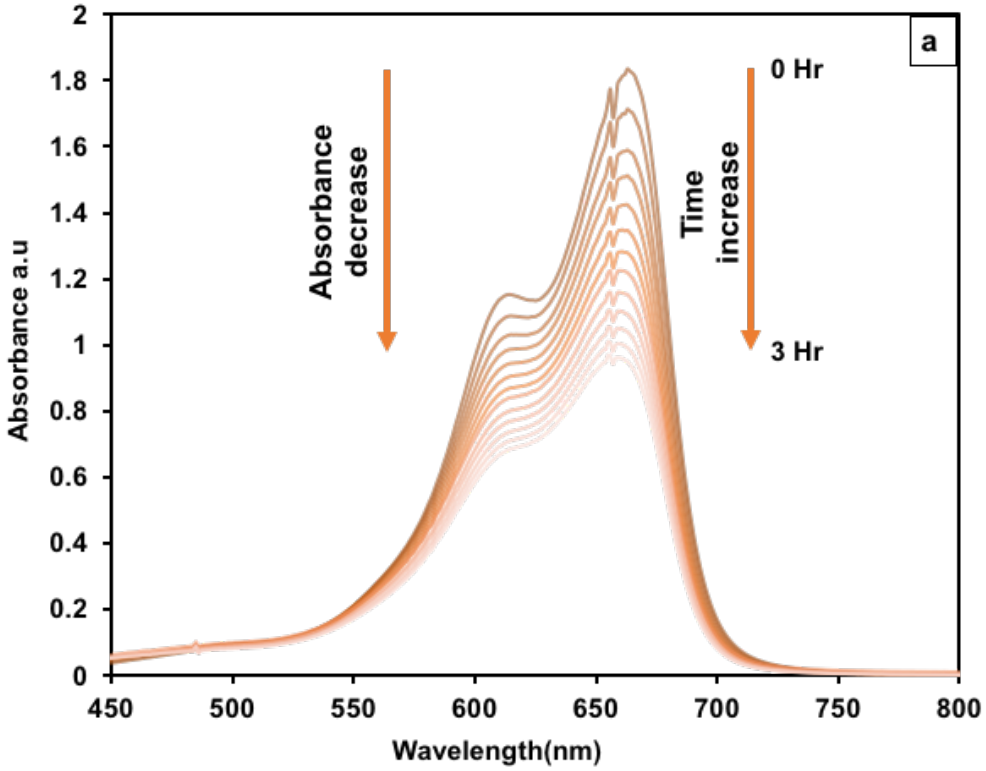
a
Absorbance decrease
Time increase
0 Hr
3 Hr
Absorbance a.u
Wavelength(nm)
2
1.8
1.6
1.4
1.2
1
0.8
0.6
0.4
0.2
0
450
500
550
600
650
700
750
800

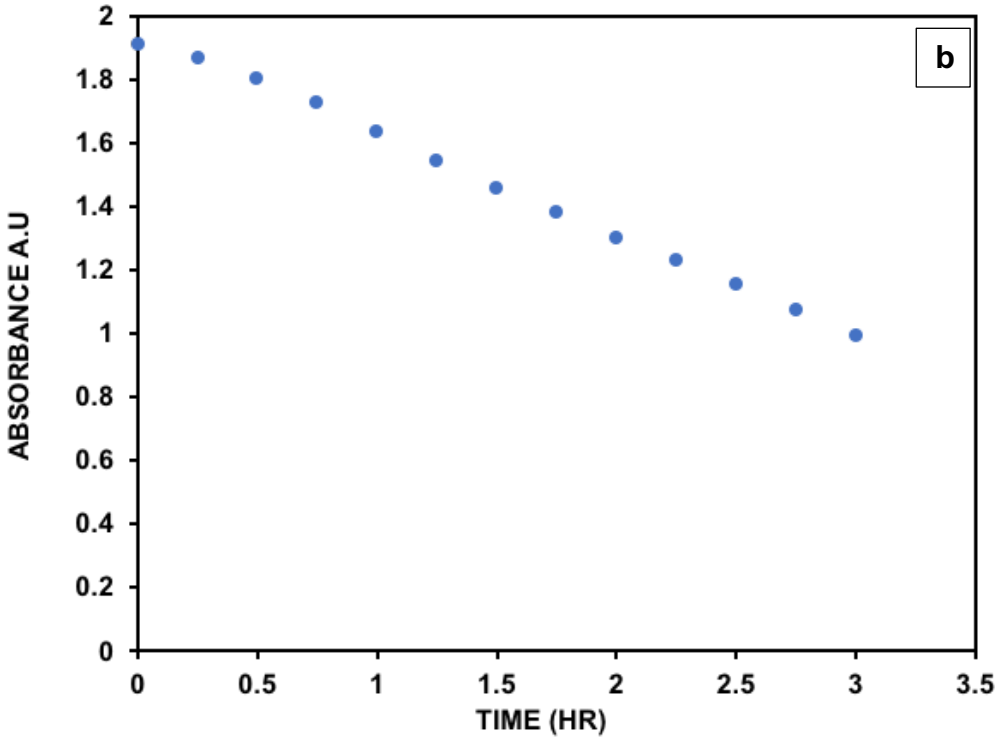
b
ABSORBANCE A.U
TIME (HR)
2
1.8
1.6
1.4
1.2
1
0.8
0.6
0.4
0.2
0
0
0.5
1
1.5
2
2.5
3
3.5

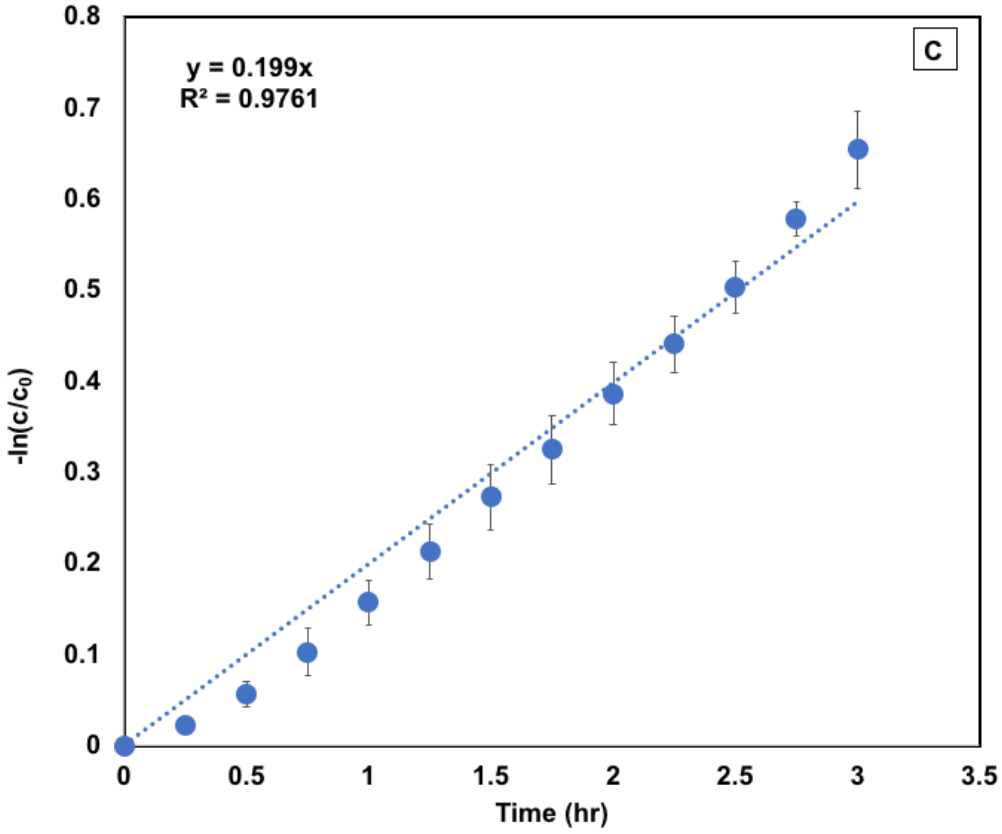

Figure 3.4 Shows (a) UV-vis absorbance spectrum for $BiVO_4$ (1 layer) film thickness (2 cm x 2 cm) film size under different solar light irradiation times in MB dye. (b) change of the absorbance data at 664 nm over time (c) the kinetic plot $ln(C/C_0)$ over time

To understand the relationship between a rate constant k_{app} and the varied factor (number of layers in figure 3.45):

First of all, UV-visible absorbance spectrum data vs time was plotted in a graph by excel as shown in Figure 3.4 (a), then, an absorbance values on 664 nm (wavelength) were used to display the relationship between the absorbance and given time Figure 3.4 (b).

To confirm fitting data to Langmuir Hinshelwood model work in this system ,the kinetic study -ln (C_t/C_0) was plotted vs time, based on LH kinetic equation[7]:

$$\ln (C_t/C_0) = kKt = k_{app}t \quad \text{.....(2)}$$

Finally the rate constant will help to understand the relation between the parameter and the degradation rate.

3.3.4. Degradation of MB dye

In order to evaluate the degradation performance of MB dye with the catalyst, it's important to, 10 ml of (45μM) MB dye was exposure to visible irradiation with stirr, without catalyst .in figure 3. 5 the results show that the remediation of the MB dye slowly decreased when the irradiation time increased and did not lead to the best performance, indicating that the properties of MB are more stable without catalyst

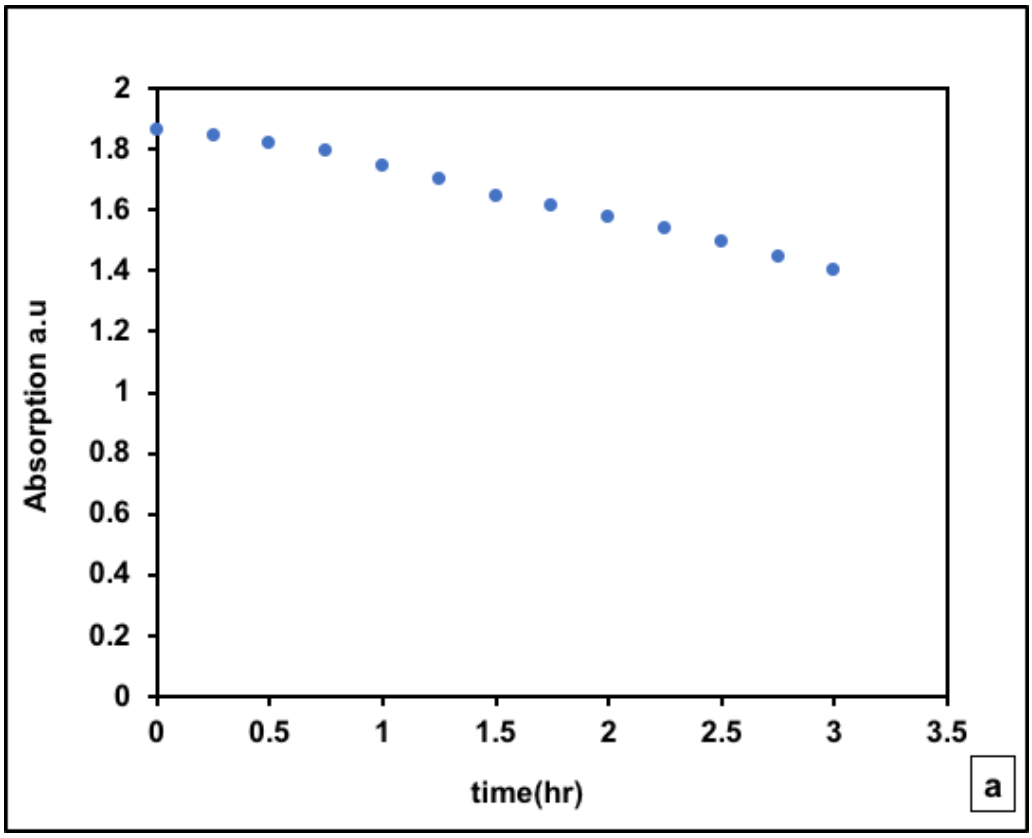
Absorption a.u
time(hr)
a

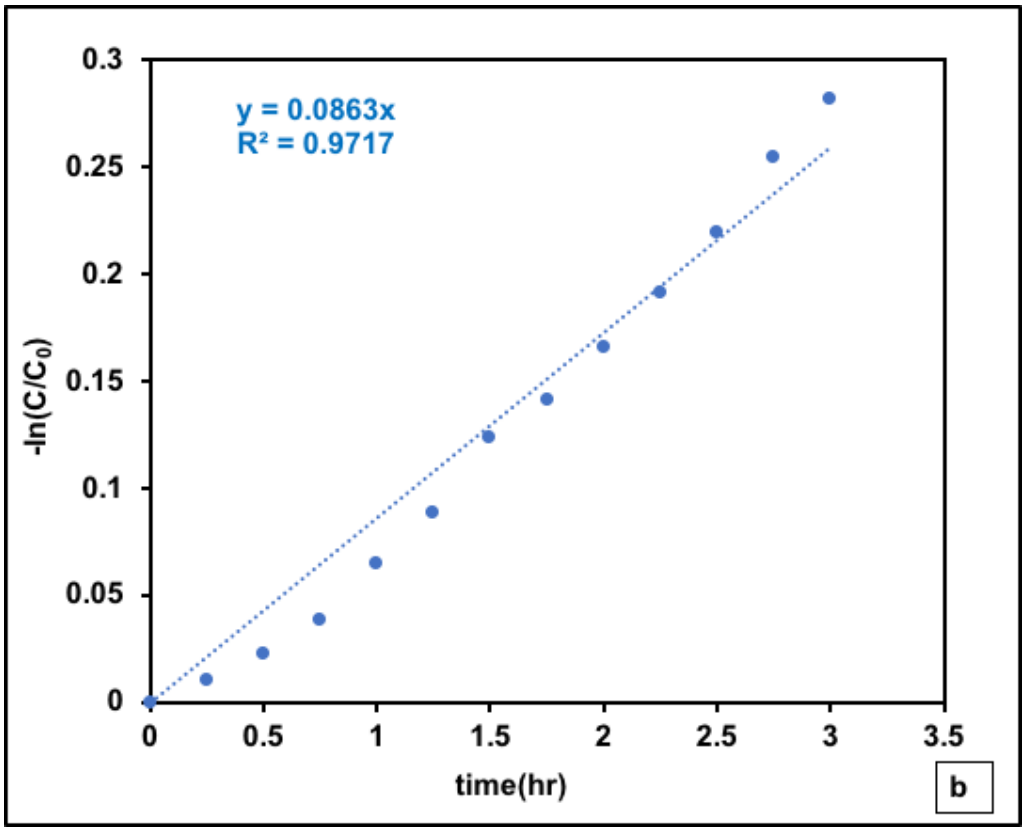
y = 0.0863x
R² = 0.9717
-ln(C/C0)
time(hr)
b

Figure 3.5 the absorption at 664 nm for MB vs time (b) kinetic study for the degradation of MB dye vs time (hr), in 10 ml reactor volume.

3.3.5. Studying the effect of changing the film thickness on the degradation rate of MB

Four different layers of each TiO_2 and $BiVO_4$ films were prepared. All layers were measured three times by Profilometer – Veeco Dektak 150 (as mentioned in Chapter 2) and the dye solution was put back to the reactor after each measurement. In the case of $BiVO_4$, the average height of each layer for both catalysts are listed below:

Number of layers	Thickness (μm)	
	$BiVO_4$	TiO_2
1	0.88 ± 0.03	0.91±0.10
2	1.30 ± 0.05	1.2±0.2
3	2.0 ± 0.04	2.93±0.03
4	2.60 ± 0.17	3.2±0.2

Table 3. 2 the average Height of each layer for both catalysts $BiVO_4$ and TiO_2, measured by Profilometer – Veeco Dektak 150

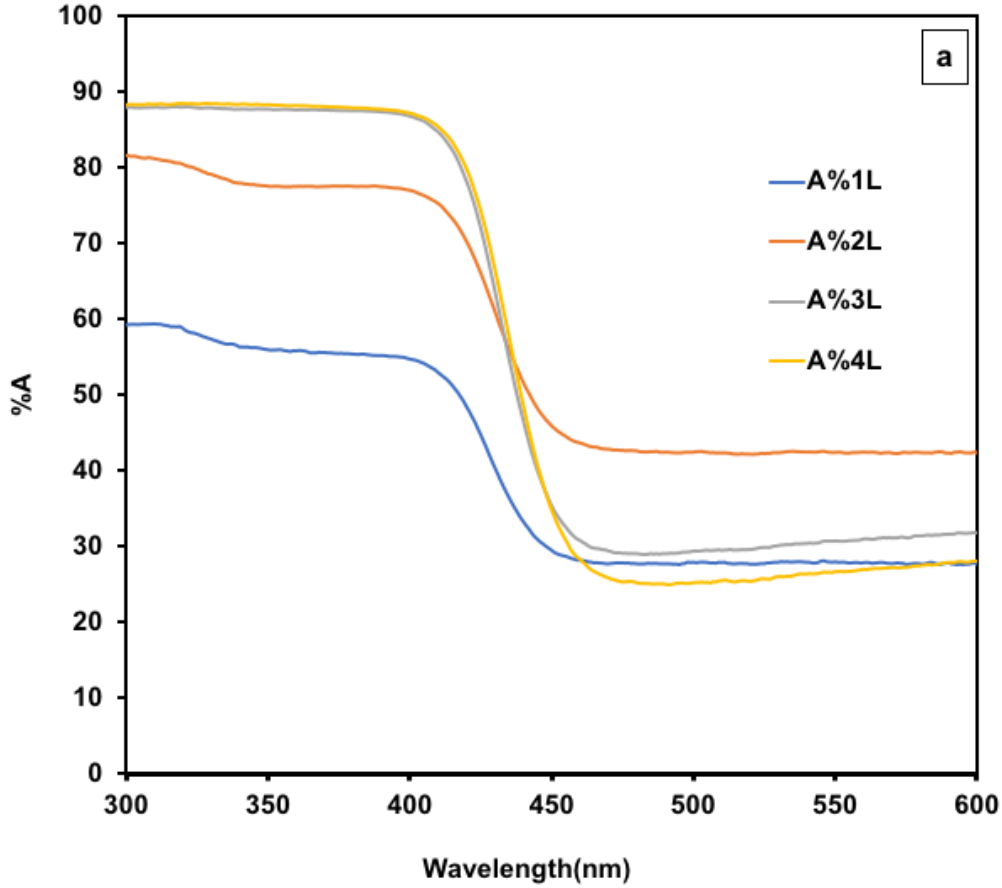
a
A%1L
A%2L
A%3L
A%4L
%A
Wavelength(nm)
100
90
80
70
60
50
40
30
20
10
0
300
350
400
450
500
550
600

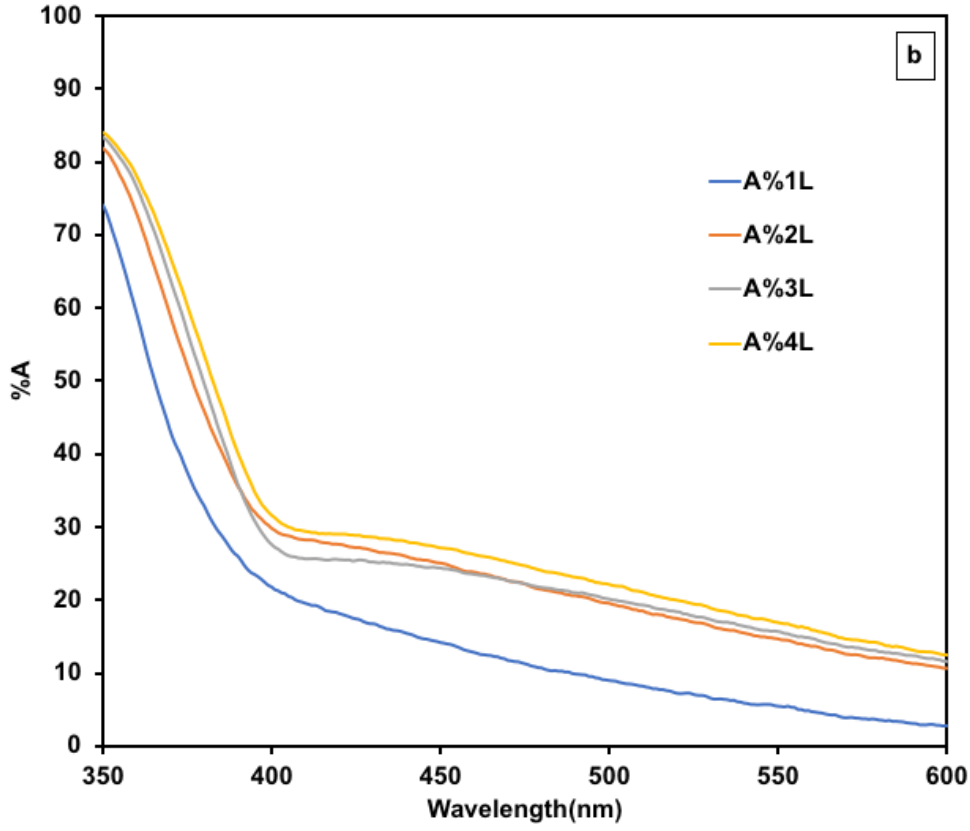
b
A%1L
A%2L
A%3L
A%4L
%A
Wavelength(nm)
100
90
80
70
60
50
40
30
20
10
0
350
400
450
500
550
600

Figure 3.6 UV-vis diffuse (a) absorption spectra for $BiVO_4$ in the range of 350–400 nm (b) absorption spectra for TiO_2 in the range of 350–400 nm

The results in figure 3.~~5~~6(a) and (b) of TiO_2 and $BiVO_4$ films, Respectively, indicate that the absorbed light in is in the range 350 to 400 nm for two layers film thicknesses is higher than one layer and the three layers is higher than one and two layers and the film which has four layers has a bigger absorbance percentage. The transmittance and reflectance results were ~~tested~~ measured by an integrating sphere spectrophotometer, and the results of the shape of the absorbance agreed well to the literature reported by Khade et al[8] and Kite et al[9] that the spectra of TiO_2 films showing strong absorption below 400 nm , which corresponding to the bandgap energy of TiO_2 (3.2 eV).

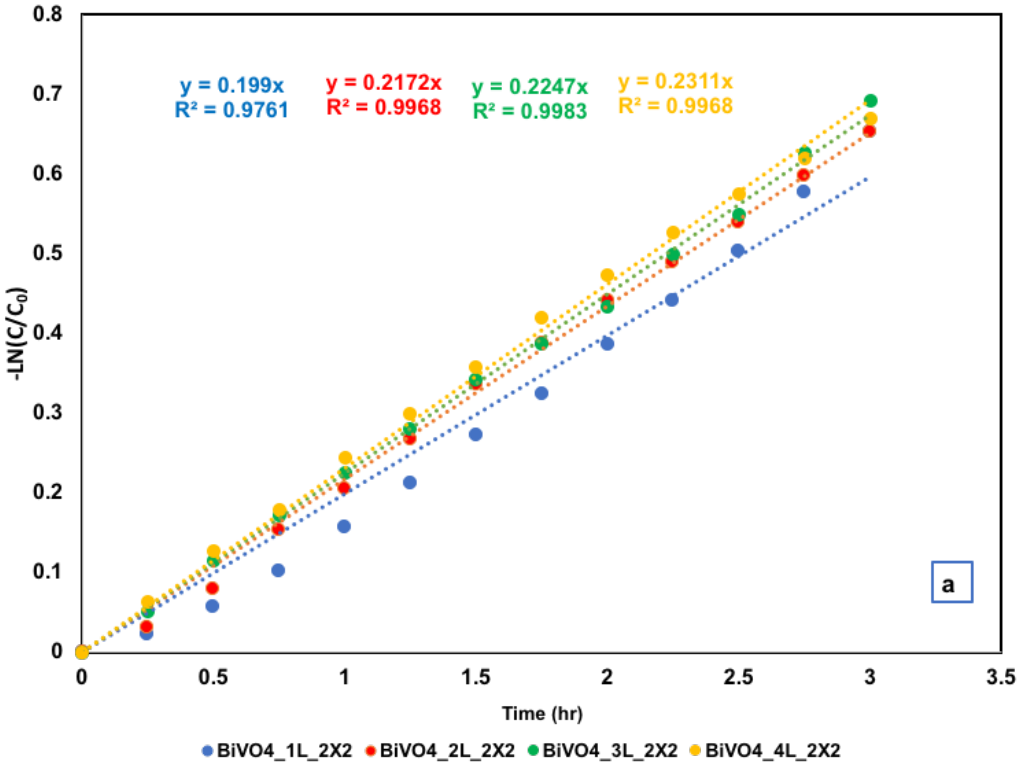

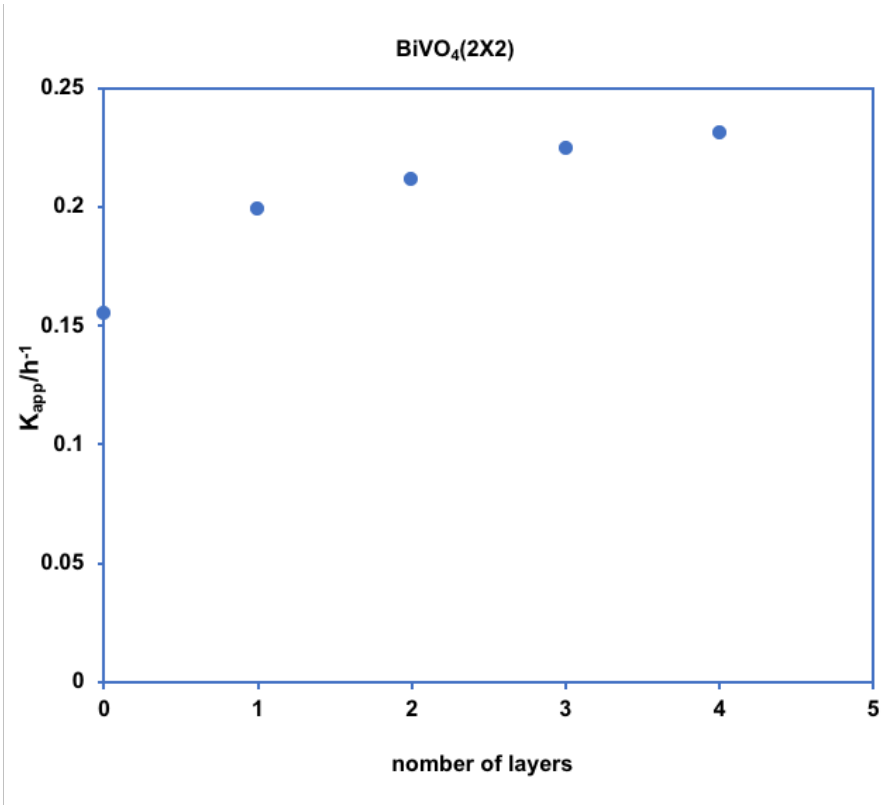

Figure 3.7 (a) The kinetic plots (- lnC/C_0) vs time. (b) The relationship between rate constant Kapp and number of layers for $BiVO_4$.

Furthermore, as shown in figure 3.67 (a), a linear relationship can be observed when plotting-ln(C_t/C_0) as a function of time using Langmuir–Hinshelwood (LH) equation:

$$\ln(C_t/C_0) = kKt = k_{app}t \quad [10]$$

Where $k_{app}t$: rate constant. -ln(C_t/C_0) as a function of lighting time which display a linear relationship as a straight line with slope corresponding[8]. By plotting values of the slope of the previous figure 3. 7(a) as a function of the film thickness the degradation rate increases continuously by increasing the film thickness figure 3.7(b) as a result of raising the total surface area in addition to the photocatalytic loading[11] which caused Increase the light harvesting and the total photocatalyst surface , thus generating more electron and hole pairs [12]

The measurements in figure 3.8 (a) confirmed that the relation between -ln (C_t/C_0) Vs time were fitted to the pseudo-first-order and fitted to the LH models (equation 2).

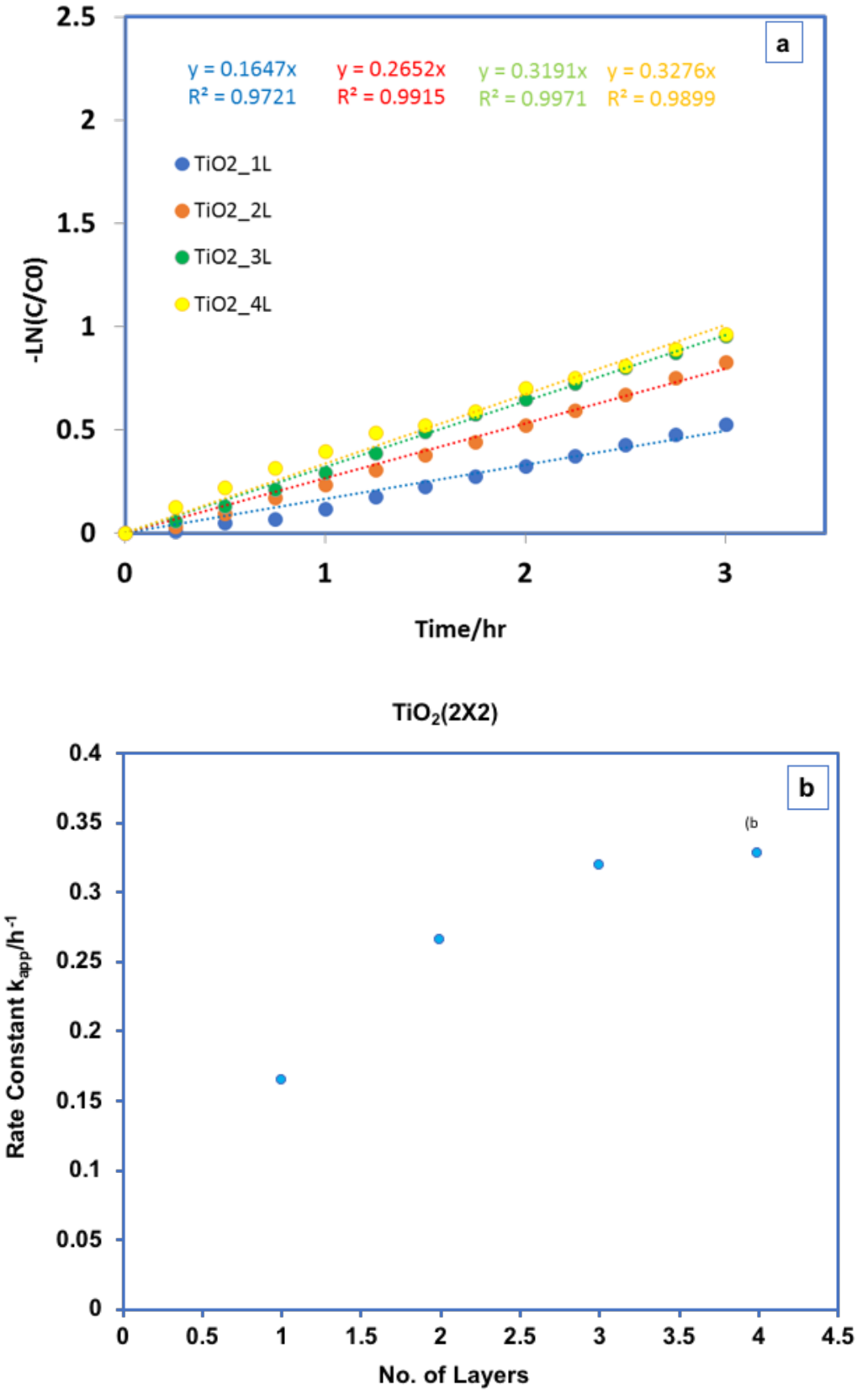

Figure 3.8 (a) the relationship between a kinetic study for the degradation of MB dye over the TiO_2 (1 layer) films, (2 cm X 2 cm) film

area for four different film thicknesses (1 layer, 2 layers, 3 layers, 4 layers) over time. (b) The rate constant vs film thicknesses (1 layer, 2 layers, 3 layers, 4 layers) over time. (b) The rate constant vs film thicknesses for TiO_2 for four different layers (1, 2, 3 and four layers) for (2 cm X 2 cm) film size.

In figure 3.8(b) the degradation rate was increased with increasing TiO_2 film thickness according to the rise in the semiconductor's molecules, therefore, increase the absorbed sites and the hydroxyl ions which then enhances the availability of electron-hole reactions[13].

Furthermore, there was a more pronounced thickness dependence of the degradation rate for TiO_2 than $BiVO_4$.

3.3.6. Studying the effect of changing the reactor volumes on the degradation rate of MB model dye

Reactor volume is one of the parameters that can be expected it has a direct impact on the photodegradation rate of investigated dye solutions[14]. For this purpose, series of reactors with different volumes were made to vary the reactor volumes which are: (5ml, 10ml, 20ml, 50ml, and 100ml), as one of the essential experiments to study the variance in degradation rate and evaluate the effect of changing the reactor size on photodegradation rate of MB the model dye using two photocatalysts films: TiO_2 and $BiVO_4$. Other testing conditions were kept constant including MB concentration(45 μM), film thickness (0.88 ± 0.03) μm for $BiVO_4$ and (0.91±0.1) μm for TiO_2, film size(2 cm X 2 cm) , light intensity (100 mW cm^{-2}) and the reaction temperature (25°C).

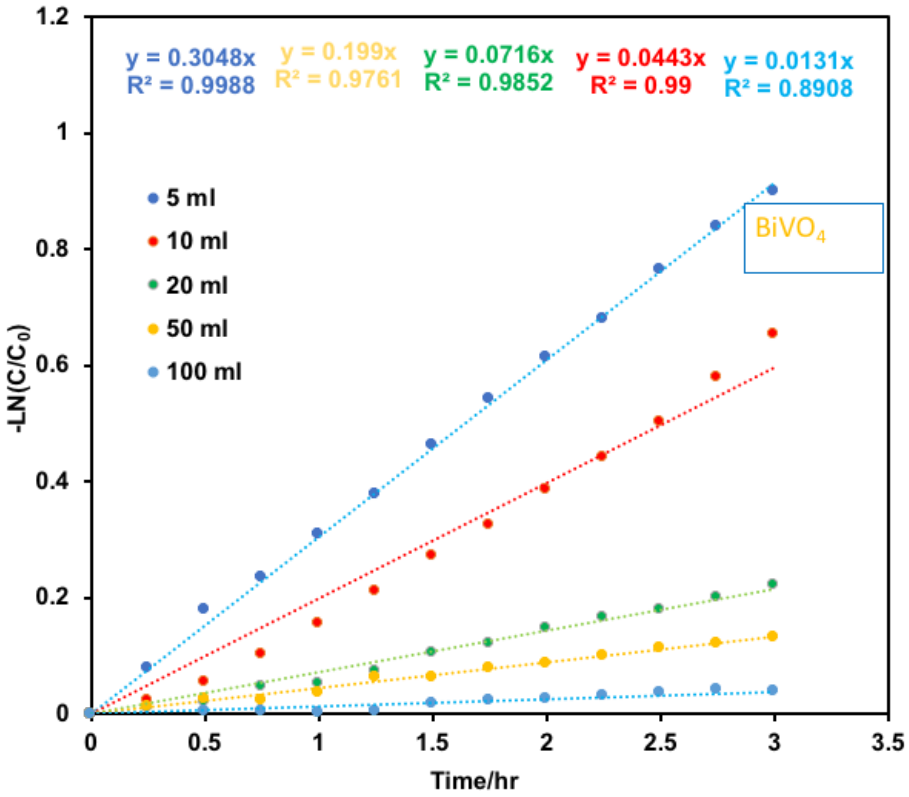

Figure 3. 9 Comparison of kinetic plots ln(C_t/C_0) vs t, for degradation of MB using $BiVO_4$ film (2 cm x 2 cm) under solar light irradiation in different reactor volumes (5 ml, 10 ml, 20 ml, 50 ml, 100 ml). Light intensity is 100 mW cm^{-2}

In figure 3.89 the data indicated that the data was fitted to the pseudo-first-order Langmuir Hinshelwood model because the relation between ln (C_t/C_0) vs time was linear.

However, low reactor volume such as 5 and 10 ml shows higher degradation rate compared to larger reactor volume, assume the same number of radicals generator (AOP).

Hence the same number of the dyes per unit time is destroyed, but the larger reactor has more dye present, hence the rate is lower. This should provide a mathematical model for the relationship between k_{appt} and volume.

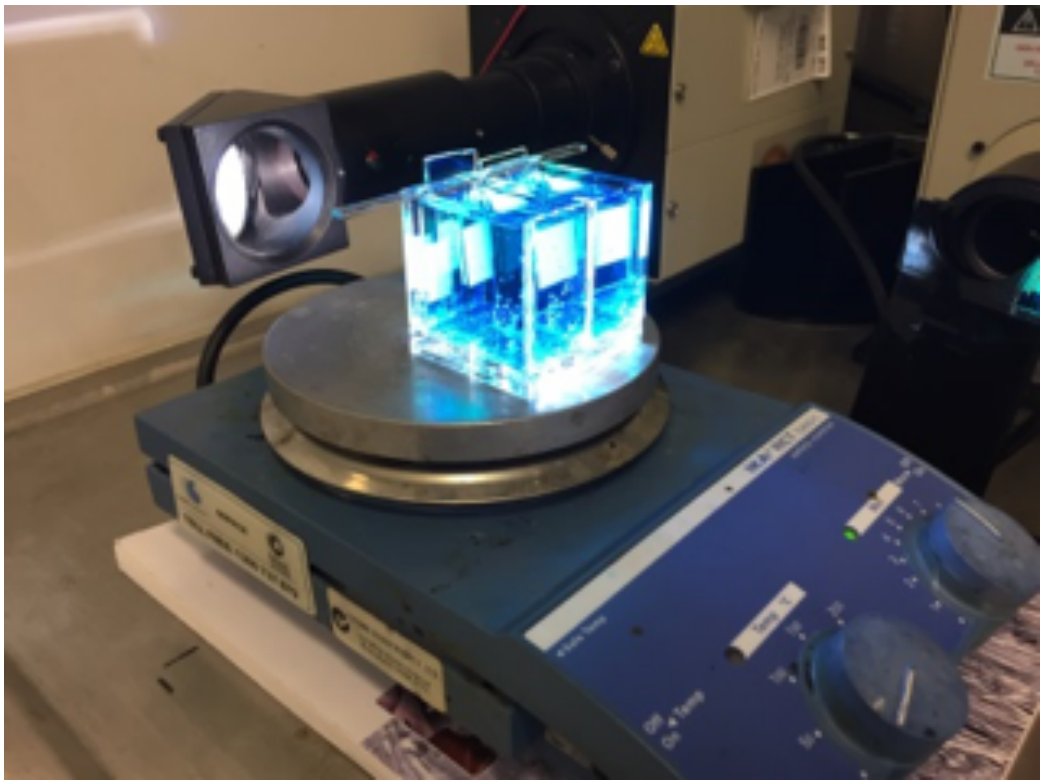

Figure 3.10 image of set up of the 50 ml reactor designed in this study

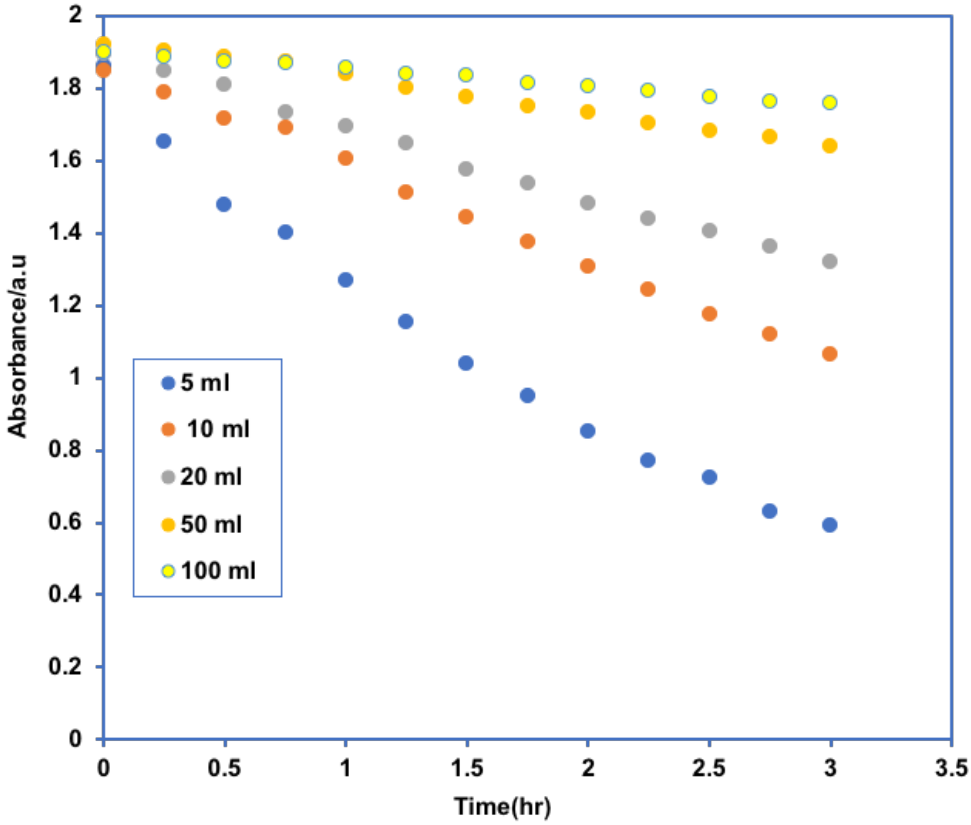
Absorbance/a.u
Time(hr)
5 ml
10 ml
20 ml
50 ml
100 ml

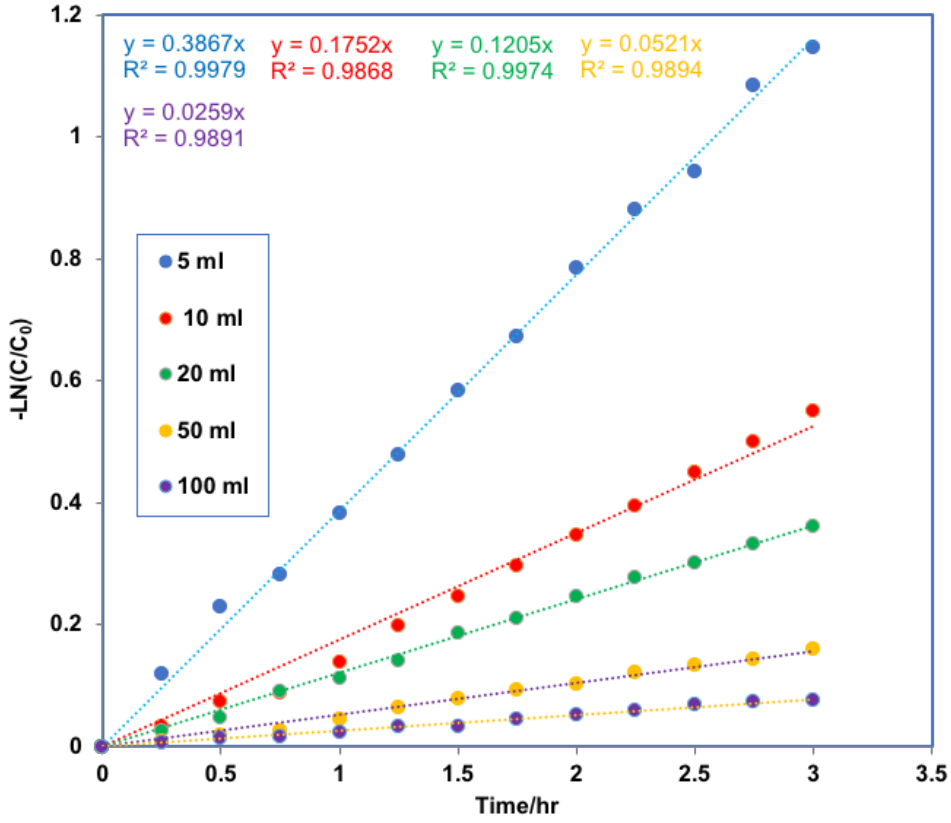
y = 0.3867x
R² = 0.9979
y = 0.1752x
R² = 0.9868
y = 0.1205x
R² = 0.9974
y = 0.0521x
R² = 0.9894
y = 0.0259x
R² = 0.9891
-LN(C/C0)
Time/hr
5 ml
10 ml
20 ml
50 ml
100 ml

Figure 3. 11 (a) the absorption at 664nm for TiO_2 vs time (b) kinetic study for the degradation of MB dye vs time (hr), for TiO_2 1 layer films thickness and (2 cm X 2 cm) film size with 100 mW cm^{-2} light intensity, for different reactor volumes (5 ml, 10 ml, 20 ml, 50 ml, 100 ml), 100 mW cm^{-2} light intensity, 1 layer thickness, 45 µM MB.

The decrease of MB dye absorption in the presence of TiO_2 films are shown in figure 3.11.a. As it can be seen, an important change of MB absorption happened with 5 ml reactor volume while it's less effective with 10 ml reactor volume.

The relation between ln (C/C_0) over the time is showing a linear relationship, which can fit LH models, as shown in figure 3.11 b.

Figure 3.12 displays a linear relationship for changing the degradation rate based on altered reactor volumes. This means that decrease the reactor volume leads to increase the degradation rate. By varying the reactor volumes to 100 ml, the degradation rate has been decreased to a quarter of 5 ml reactor due to increasing the number of dye molecules but the photocatalyst amount still the same which means increase the availability of active sites on the surface of photocatalytic[16].

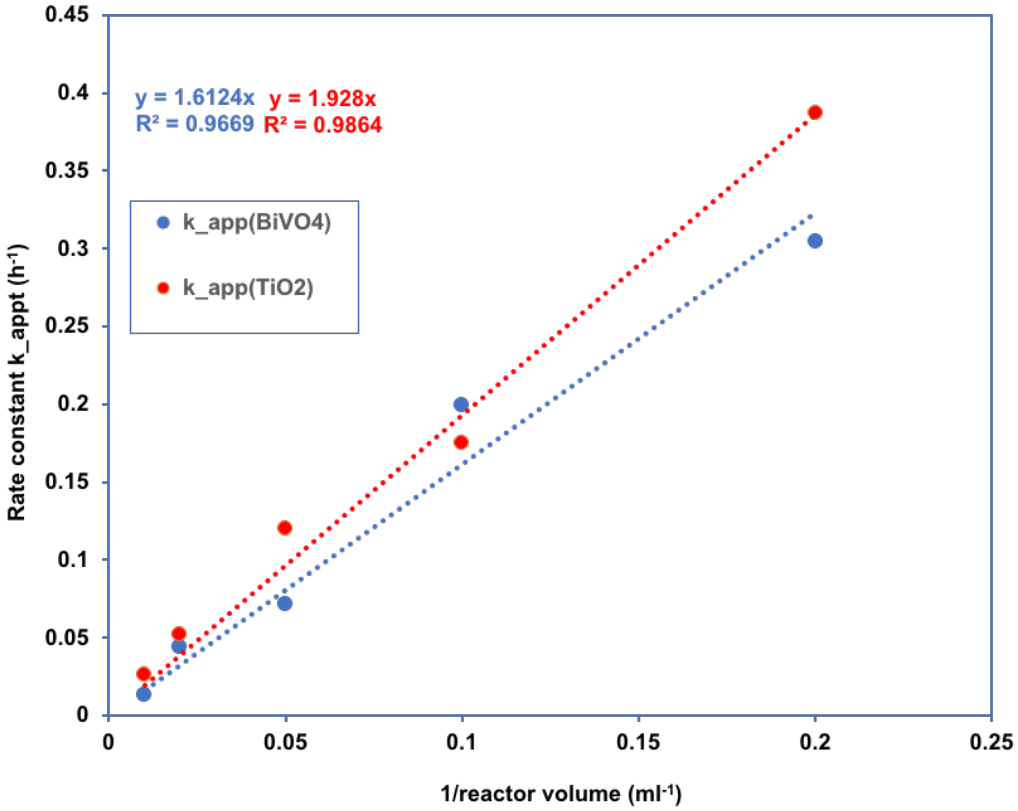

Figure 3.12 Change in the rate constant ($K_{app}t/h^{-1}$) with the 1/V (reactor volume) for two photocatalyst films, TiO_2 and $BiVO_4$. In 1-layer film thickness and (2 cm X 2 cm) film size with 100 mW cm^{-2} light intensity, ~~at~~ for different reactor volumes (5 ml, 10 ml, 20 ml, 50ml, 100 ml), 100 mW cm^{-2} light intensity, 1-layer thickness, 45 µM MB

3.3.7. Studying the effect of changing the film size on the degradation rate of MB

Four different sizes of TiO_2 films were prepared including (2 cm X 1 cm), (2 cm X 2 cm), (2 cm X 3 cm), (2 cm X 4 cm), and keep the other factors such as MB concentration(45 µM), film thickness (0.88 ± 0.03) µm for $BiVO_4$ and (0.91±0.1) µm for TiO_2, light intensity (100 mW cm^{-2}) and the reaction temperature (25°C) constant ,to study the effect of the changing film sizes.

Figure 3.13(a) shows linear behaviour when plot $\ln(C/C_0)$ vs time, which can fit to LH model.

In figure 3.13(b) shows the almost linear relation between the rate constant and the size of the film, which can explain as an increase the surface area of $BiVO_4$ film was led to increasing dye degradation, because of that more light harvested create more electron-hole pairs and create more radicals, Therefore, an increase in the degradation rate [17] as shown in figure 3.13 (b).

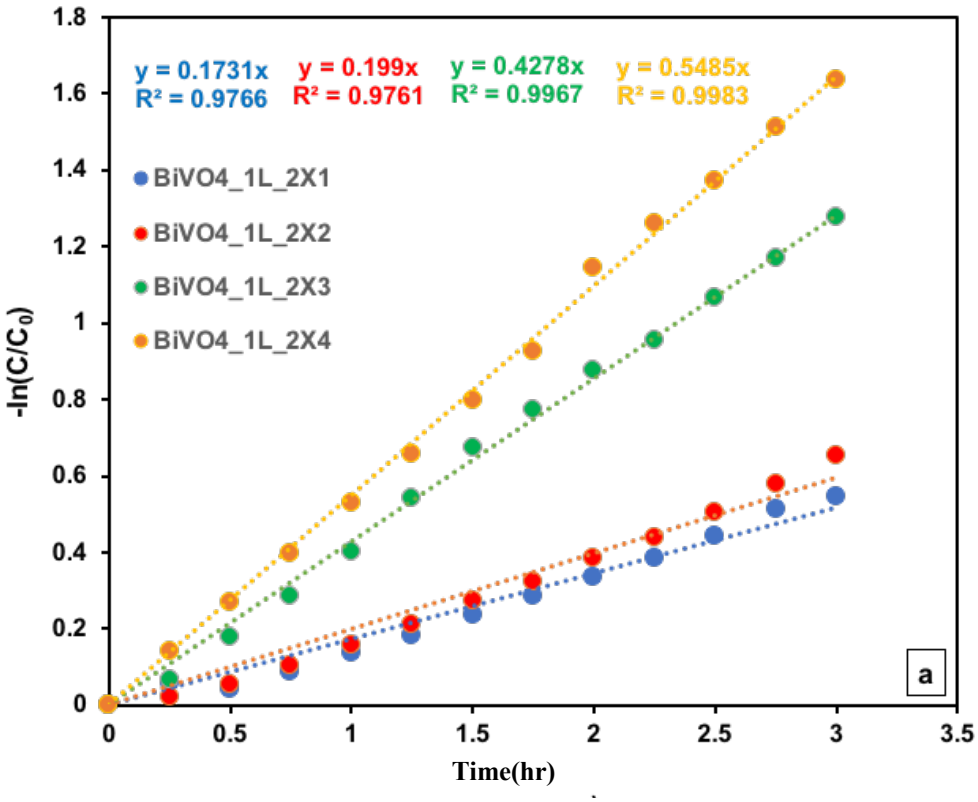

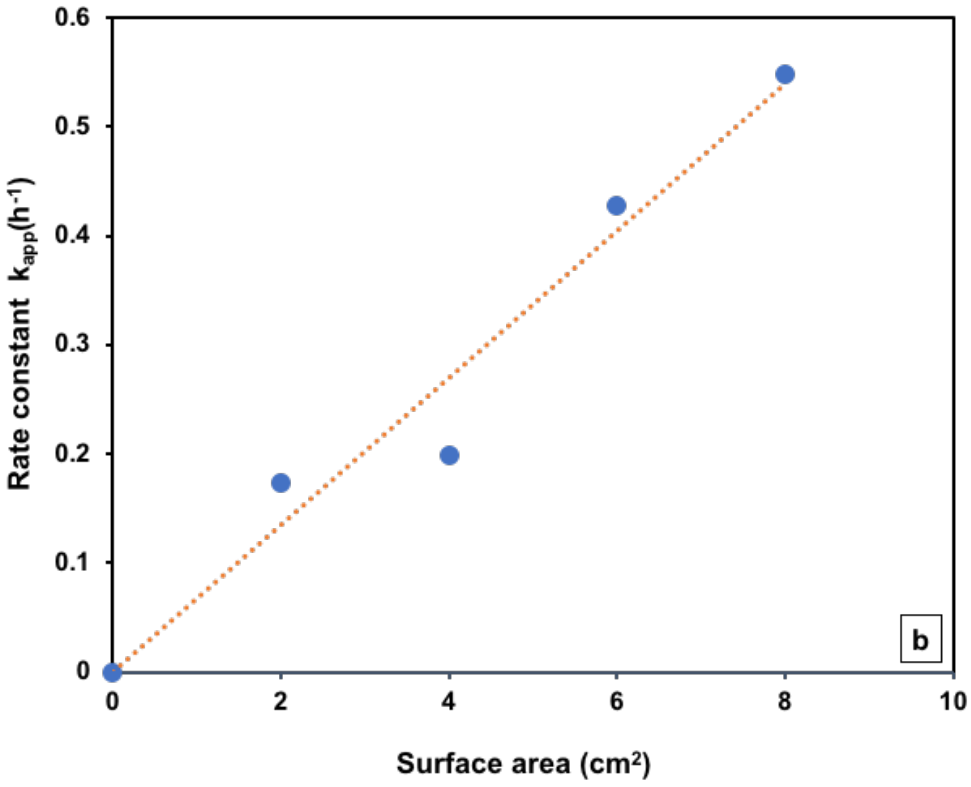

figure 3. 13 The relationship between (a) kinetic studies for the degradation of MB dye over the $BiVO_4$ (1 layer) films for four different film sizes and no catalyst , (2 cm X 1 cm), (2 cm X 2 cm), (2 cm X 3 cm), (2 cm X 4 cm) over time, (b) Rate constant ($K_{app}t/h^{-1}$) vs surface area (cm^2)for $BiVO_4$ for one layer and different film sizes, no film , (2 cm X 1 cm), (2 cm X 2 cm), (2 cm X 3 cm), (2 cm X 4 cm), 25 °C reaction temperature, 100 mW cm^{-2} light intensity, (45 µM) MB dye concentration

Figure 3.14 (a) shows that $\ln(C/C_0)$ can be fitted to LH model, and the rate constants were slightly increasing with increase the surface area, due to increasing the suspensions of the photocatalytic films as a result of over amount of $BiVO_4$ particles in the MB dye solution [18].

Figure 3.14(b) shows increase the rate constant with respect time ,the relation is nearly linear, which cause by increase the absorbed sites on the

TiO_2 surface due to increase the surface area, which means more free hydroxyl radicals which employed in dye degradation processing [19].

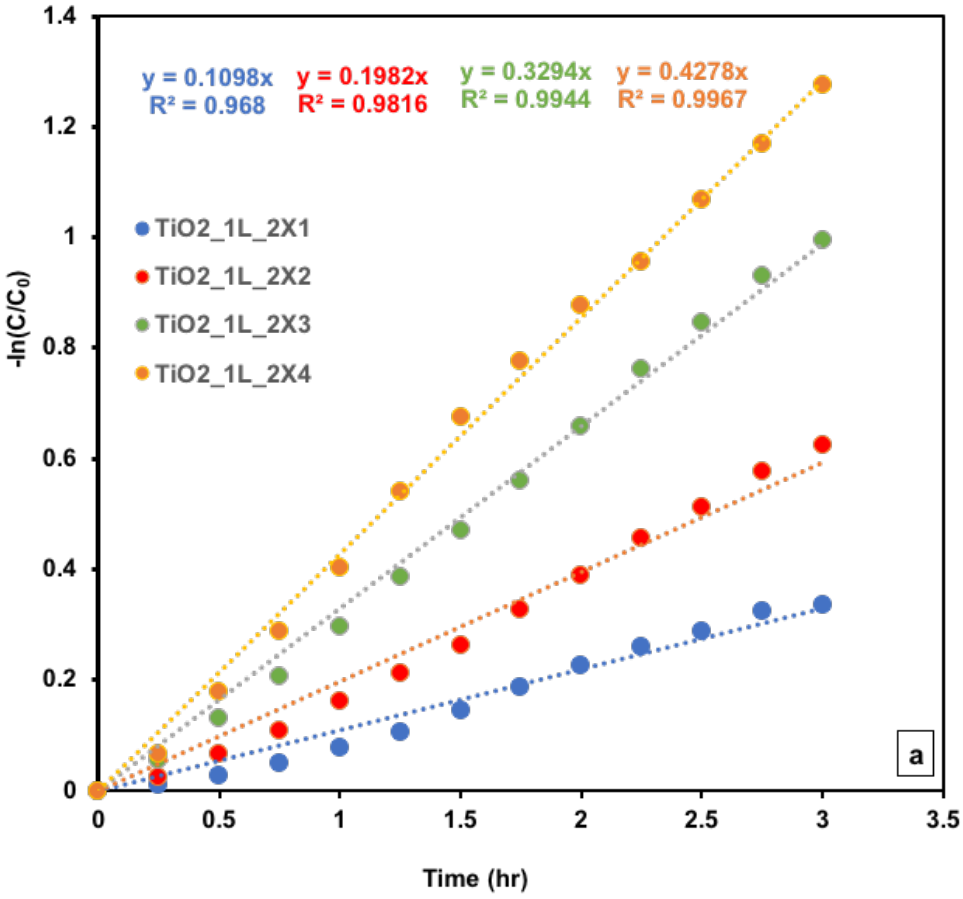
y = 0.1098x
R² = 0.968
y = 0.1982x
R² = 0.9816
y = 0.3294x
R² = 0.9944
y = 0.4278x
R² = 0.9967
TiO2_1L_2X1
TiO2_1L_2X2
TiO2_1L_2X3
TiO2_1L_2X4
-ln(C/C0)
Time (hr)
a

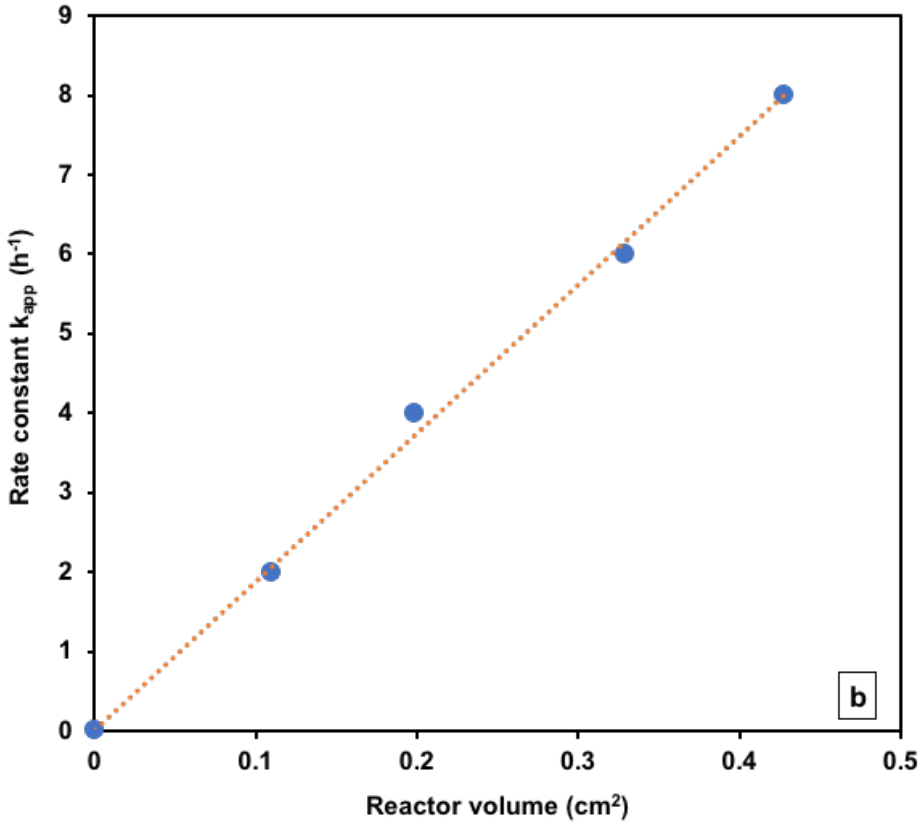
Rate constant kapp (h-1)
Reactor volume (cm2)
b

Figure 3. 14 the relationship between a kinetic study for the degradation of MB dye over the TiO_2 (1 layer) films for four different film size (2 cm x 1 cm), (2 cm x2 cm), (2 cm x,3 cm), (2 cm x 4 cm) over time, B. Rate constant ($K_{app}t/h^{-1}$) ~~vis~~ vs surface area .cm^2 for TiO_2 for one layer film thickness ~~in~~ and different film sizes (2 cm x 1cm), (2 cm x 2 cm), (2 cm x 3 cm), and (2 cm x 4 cm).), 25°C reaction temperature, 100 mW cm^{-2} light intensity, (45 µM) MB dye concentration.

3.3.8. Studying the effect of changing the light intensity on the degradation rate of MB model dye~~:~~

The solar stimulator (LCS-100TM ORIEL®) with an AM1.5G filter was used to illuminate the reactor during the photodegradation process. The effects of increasing illumination intensity were investigated in this study, the light intensity was controlled by change the distance between the lamp power and the reactor, the minimum light intensity applied was 10 mW cm^{-2} and the maximum 250 mW cm^{-2} ,while the, MB concentration(45 µM), film thickness (0.88 ± 0.038) µm for $BiVO_4$ and (0.91±0.1) µm for TiO_2, film size (2 cm X 2 cm), reactor volume (10 ml) and the reaction temperature (25°C) were kept constant. . The effect of the light intensity on the photocatalytic degradation rate of MB dye in the presence of $BiVO_4$ film was investigated in figure 3.14 (a) and it clearly shows almost linearly relationship with the time and fitted to the pseudo-first order (Langmuir–Hinshelwood model) [8]:

$\ln (C_t / C_0) = - k_t$ ……. (2)

In figure 3.125. b, the rate constant (k) was increased with increasing the light intensity around (10,25,50,75,100,150,200,250) mW cm^{-2} due to increase the light photons which raises the possibility to generate the hole-electron pairs and enhances the dye removing reaction [20].

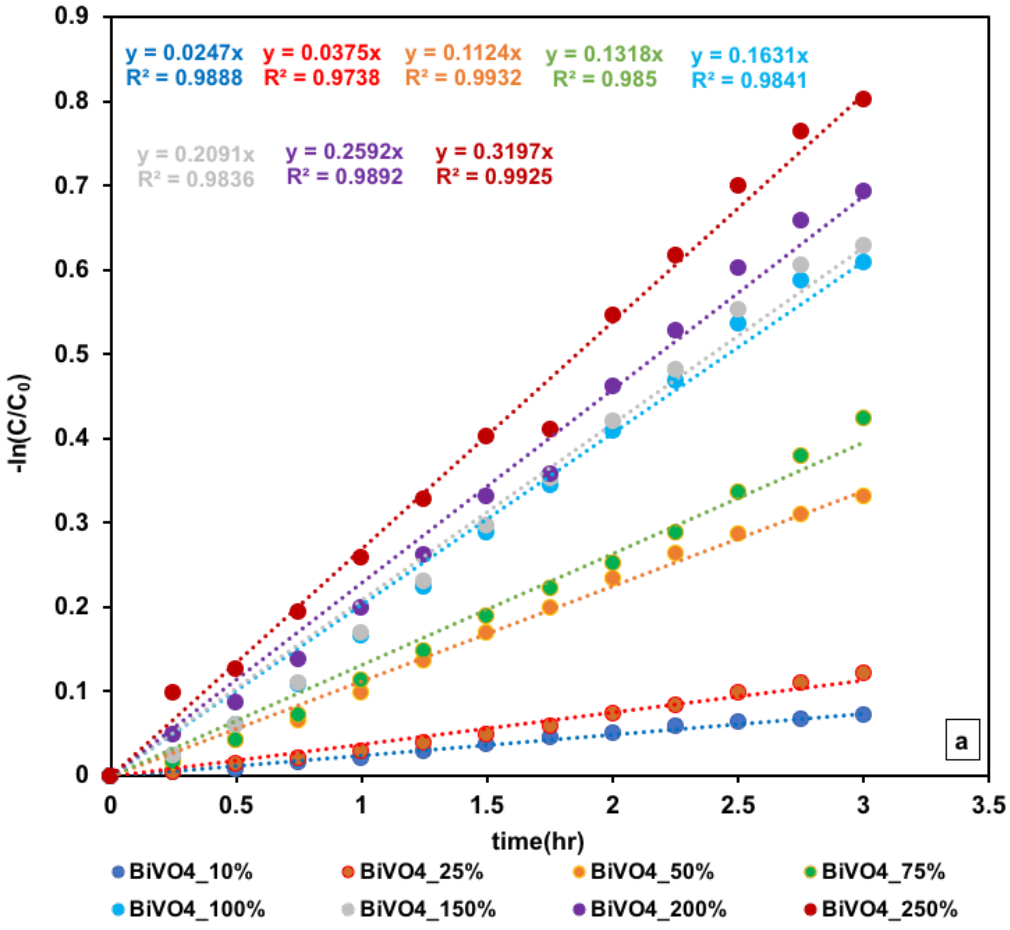

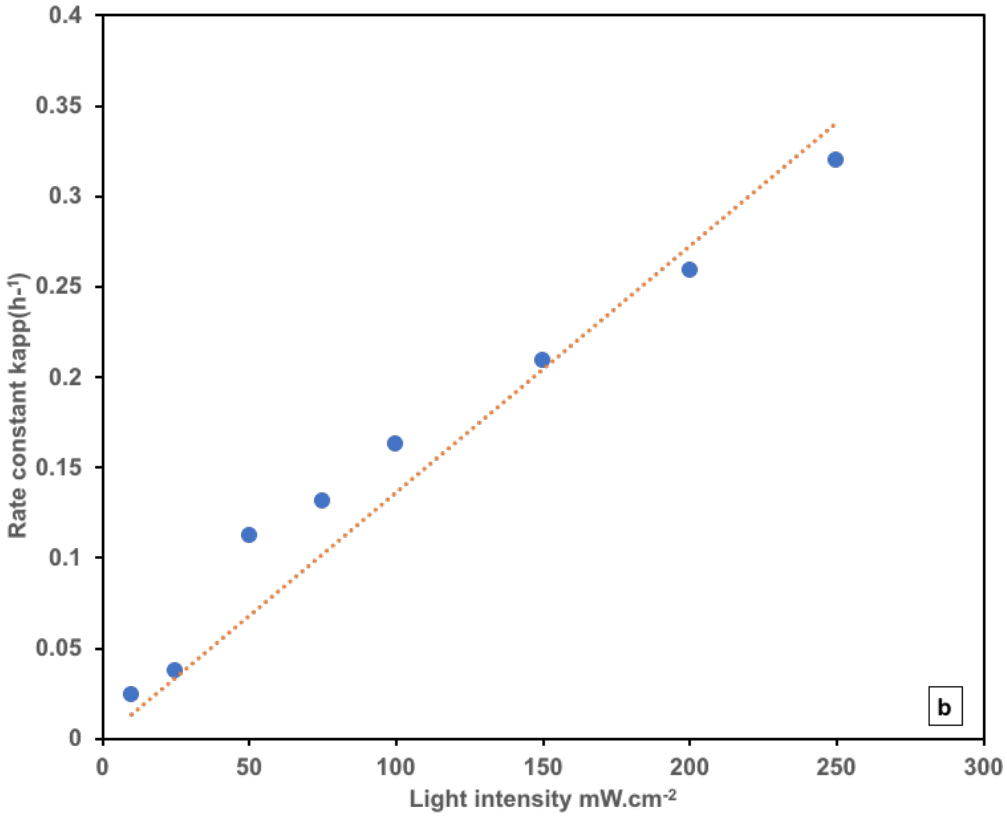

Figure 3. 15 A. kinetic study for the degradation of MB dye over the $BiVO_4$ (1 layer) films over the time. B. the average ~~of~~ degradation rate ($K_{app}t/h^{-1}$) for $BiVO_4$ at different light intensities (10 mW cm^{-2}, 25 mW cm^{-2}, 50 mW cm^{-2}, 75 mW cm^{-2}, 100 mW cm^{-2}, 150 mW cm^{-2}, 200 mW cm^{-2}, 250 mW cm^{-2}). (2 cm x 2 cm) film size, (25°C) reaction temperature, (45 µM) MB dye concentration.

As can be noticed in figure 3.16 (a), there is a linear relationship between ln (C/C_0) over the time, which can fit to LH model.

In figure 3.1~~5~~6. b, it was evident that the degradation rate of TiO_2 more sensitive to the illumination change than $BiVO_4$. When the illumination intensity gradually changed from 50 to 250 mW cm^{-2}, the degradation rate of MB was notably improved as a result of creating more hole-electron pairs and that

leads to increased dye removal percentage.

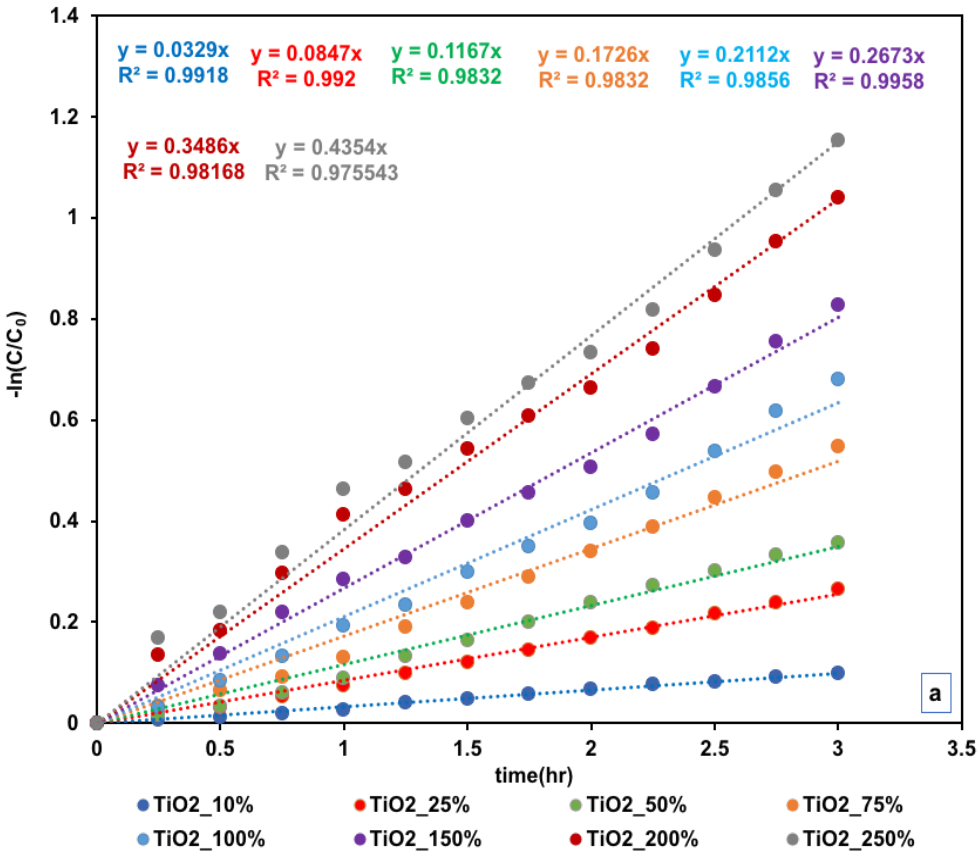

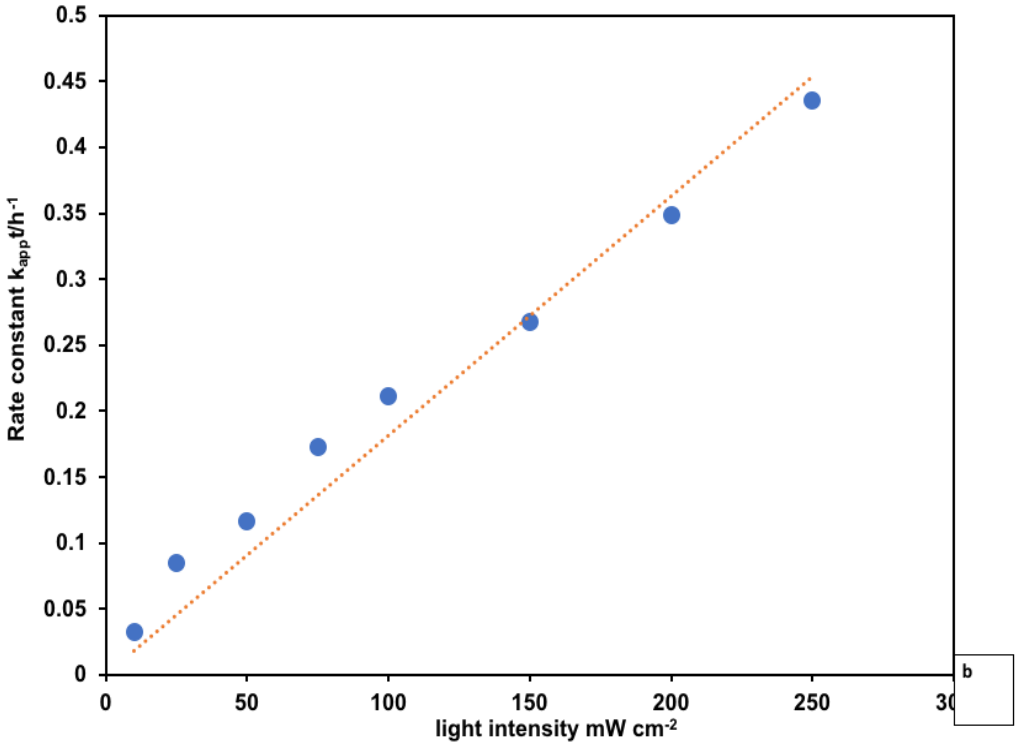

Figure 3. 16 A. kinetic study for the degradation of MB dye over the TiO_2 (1 layer) films over the time. B. the average degradation rate ($K_{app}t/h^{-1}$) for TiO_2 and different light intensities (10 mW cm^{-2}, 25 mW cm^{-2}, 50 mW cm^{-2}, 75 mW cm^{-2}, 100 mW cm^{-2}, 150 mW cm^{-2}, 200 mW cm^{-2}, 250 mW cm^{-2}). (2 cm x2 cm) film size, (25°C) reaction temperatures, (45 µM) MB dye concentration.

3.3.9. Studying the effect of changing the reaction temperature on the degradation rate of MB

The reliance of MB dye degradation rate on a series of reaction temperature ranged between 2-5°C, 25, 35 and 50°C was investigated in this research using the cooler and heater system which were mentioned in the chapter (2). All other parameters such as, MB concentration(45 µM), film thickness (0.88 ± 0.038) µm for $BiVO_4$ and (0.91±0.1) µm for TiO_2, film size (2 cm X 2 cm) , reactor volume (10 ml) and the reaction temperature (25°C) were kept constant.

The reaction cooled down to about (2°C – 5°C) for each of $BiVO_4$ and TiO_2, the results are presented graphically in figure 3.17 and figure 3.18, respectively. There was a linear relationship formed by plotting $\ln(C_t/C_0)$ as a function of irradiation time as seen in figure 3.17 (a). It has been found that, increasing reaction temperature from 5 to 50 °C increased the kinetic energy of the dye molecules (reactants). In turn, increases the adsorption of these molecules on the photocatalyst surface and reveal effective photo-degradation of MB[21].

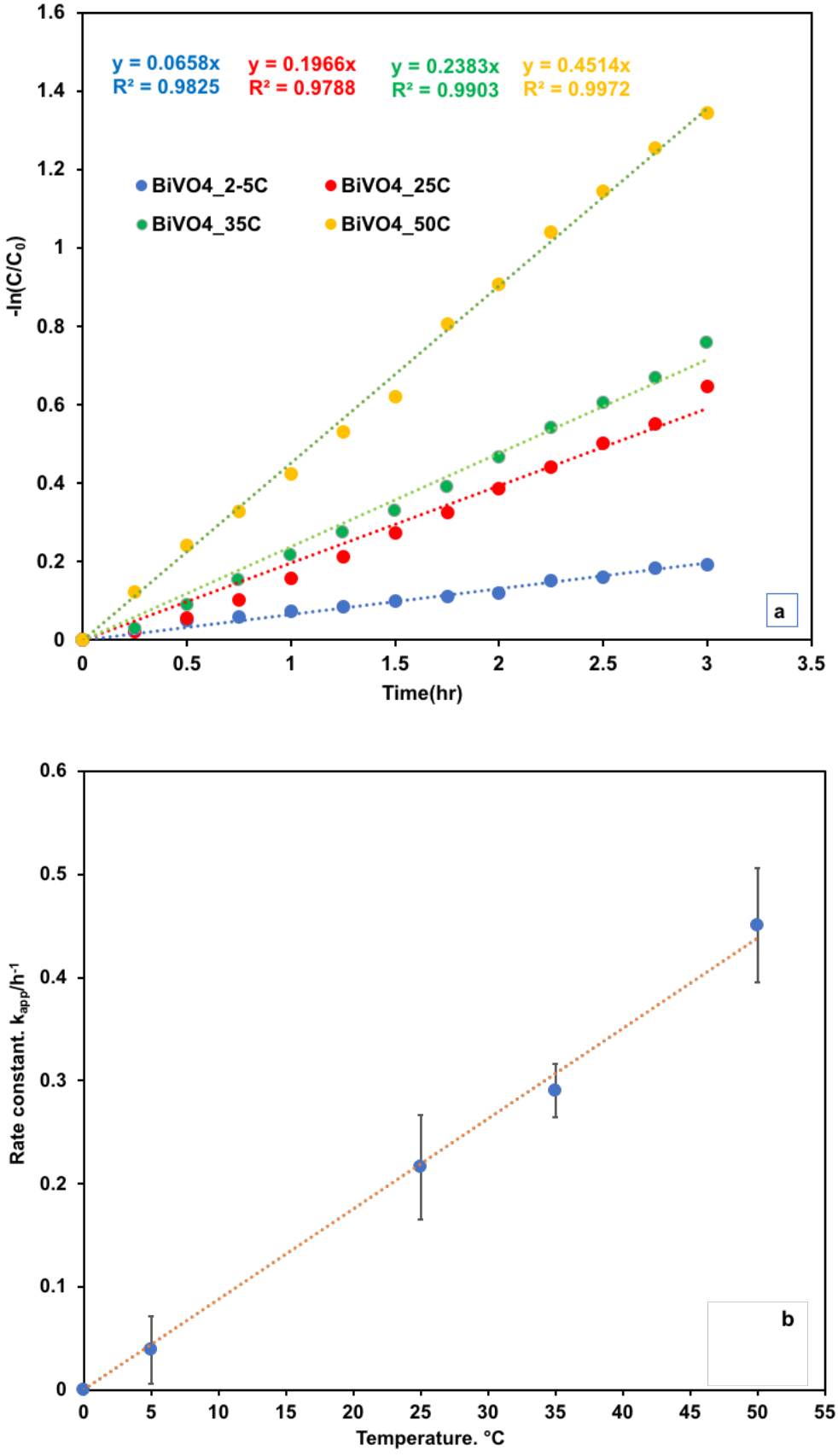

Figure 3. 17 a. kinetic study for the degradation of MB dye over the

BiVO4 (1 layer) films over time. B. Average degradation rate (k_{app}/h^{-1}) for $BiVO_4$ at different temperatures (2-5°C, 25, 35 and 50°C), (2 cm x2 cm) film size ,100 $mW.cm^{-2}$ and 1-layer film thickness

In figure 3.18 a, linear relationship was seen of kinetic over specific given time. (Figure 3.18 b), heating up the reaction to 50°C showed same performance of previous catalyst $BiVO_4$. The dye removing rate was found to increase quickly in presence of TiO_2 semiconductor when increasing the reaction temperature about (35°C and 50°C) due to increase the kinetic energy of organic molecules in the solution and enhances their adsorption onto the catalyst surface (equations 1 & 2). Figure 3.18 b was indicated linear relationship between rate constant K_{app} and applied temperature.

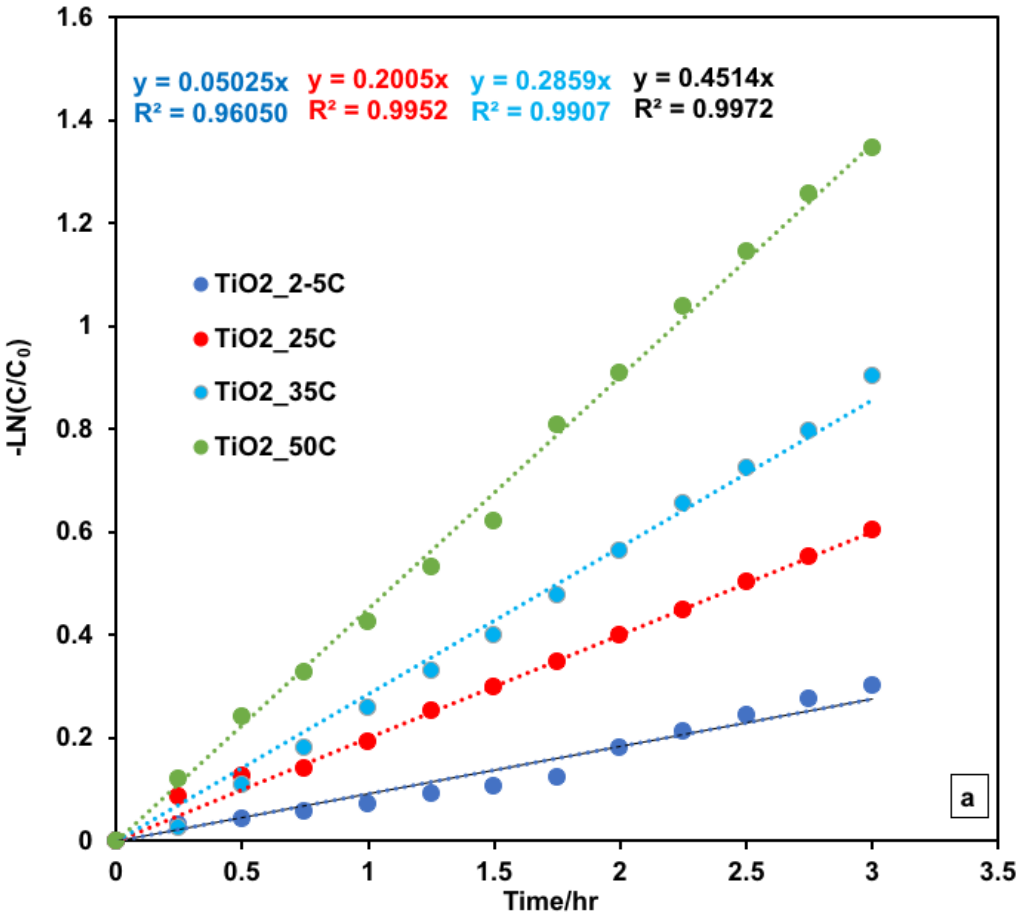

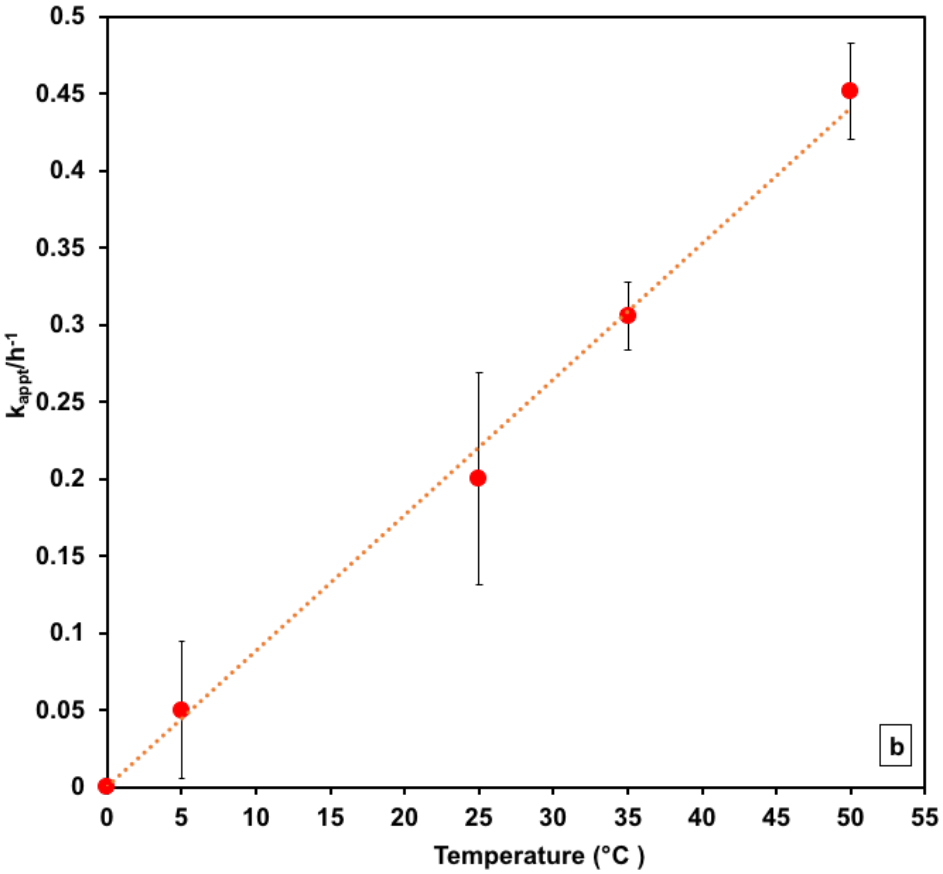

Figure 3. 18 A. kinetic studies for the degradation of MB dye over the TiO_2 (1 layer) films over the time. B. Average degradation rate (k_{appt}/h^{-1}) at a different temperature. (2 cm x 2 cm) film size ,100 $mW.cm^{-2}$,1-layer thickness Average of the degradation rate (k_{appt}/h^{-1}) at a different temperature. (2 cm x 2 cm) film size ,100 $mW.cm^{-2}$,1-layer thickness

The adsorption and desorption rates increased with temperature, showing that the dye molecules movement increased with temperature and some molecules that interact with the active sites at semiconductor's surface. Additionally, increasing the temperature will increase the diffusion of the MB dye and the diffusion of the radical spaces [22].

3.4. Conclusion:

Two photocatalysts were successfully prepared by screen-printing technology using TiO_2 and $BiVO_4$ ~~pasts~~ pastes separately. The photocatalytic performance of those two materials was studied and compared based on degradation of MB dye solutions using the solar simulator and UV-Vis light irradiation. Also, the effect of reaction conditions or factors such as initial dye concentration, reaction temperature, films sizes and thickness, and reactor volume were investigated. The testing approach included studying the effect of varying one of the factors on the degradation rate of MB while keeping the others constant. This method was repeated with the rest of the factors until all were evaluated. It has been found that the degradation rate of MB can be increased by varying reaction temperature (5, 25, 35, and 50) °C using TiO_2 and $BiVO_4$ films, however, $BiVO_4$ showed a linear relationship between the degradation rate and varied light intensities. Notably, there was a rapid increase in MB degradation after applying greater than 50 (mW cm^{-2}) of light intensity Due to the increase of the photocatalytic total surface area by increasing the loading, Subsequently, Increase the light-harvesting and generating more electron and hole pairs[23]. Varying film size has indicated a similar positive effect on obtained degradation rate which means an increased the total surface area in return.

Moreover, The absorbed light will create an electron-hole pairs which create numbers of radicals, these radicals will react with the MB dye, so can only degrade a restricted number of dye molecules per unit time.The

adsorption efficiencies of TiO_2 and $BiVO_4$ films over MB dye can be concluded based on each factor as follows:

Films thickness: increasing the number of layers of TiO_2 and $BiVO_4$ films resulted in increased absorbed light and MB degradation rate as a consequence. Actually, the 4-layers film showed a higher ability to harvest the light compared to 3, 2, &1 layers films. The 3-layers film tended to show greater harvesting than 2- and 1-layers films and so on. Furthermore, all prepared layers of TiO_2 films indicated bigger degradation rate of MB than $BiVO_4$ films which were used for the same purpose.

Reactor volume: it was found that changing the reactor volume had a linear response on adsorption efficiencies of both TiO_2 and $BiVO_4$ films over MB dye degradation. Decreasing the volume of the reactor increased the degradation of MB dye significantly in the presence of TiO_2 and $BiVO_4$ films separately. Notably, TiO_2 film revealed higher degradation of MB dye in compare to $BiVO_4$ film when the other conditions were stable but changing the reactor volume.

Film size: four sets of films dimensions were used to examine the adsorption efficiencies of TiO_2 and $BiVO_4$ film over MB dye. It's worth mentioning that, increasing the dimensions of the film led to increased degradation rate of MB dye in the system reasonably in a linear response.

Light intensity: rising the light intensity had influenced the performance of TiO_2 and $BiVO_4$ films over MB degradation. It can be said that increasing light intensity positively increased the degradation of MB using the TiO2 and $BiVO_4$ semiconductors as films. TiO_2, in specific, showed an increased degradation rate of MB dye in comparison to $BiVO_4$ films when applied for the system.

Reaction temperature: It was found that the adsorption efficiencies of TiO_2 and $BiVO_4$ films over MB dye had increased by increasing the temperature of the system. This result also interestingly showed that TiO_2 and $BiVO_4$ had close degradation rate to MB dye. In other words, TiO_2 and $BiVO_4$ films reflected an almost similar ability over MB degradation by changing the reaction temperature.

3.3.10. Figure of merit

To compare TiO_2 and $BiVO_4$ performance FOM has been collected as a following equation

$$\textbf{FOM} = \frac{\mathbf{Kapp(hr^{-1}).Area(m^2)}}{\mathbf{Solar\ Intensity(Wm^{-2}).Volume(m^3)}} \quad \textbf{* Temperature (°C)}$$

TABLE 3. 3 Figure of merit for $BiVO_4$ and TiO_2 in different conditions

The Parameter	The material	FoM (m/W.hr)				assessment
		2x1	2x2	2x3	2x4	
reactor volume (10 ml)	$BiVO_4$		19.9			$BiVO_4$ is a better material for degradation of MB than TiO_2
	TiO_2		17.5			
Film Size (cm^2)	$BiVO_4$	17.3	19.9	20.3	21.1	$BiVO_4$ is a better material for degradation of MB than TiO_2
	TiO_2	17.5	19.7	19.9	21.3	
Light Intensity 100%	$BiVO_4$		18.31			TiO_2 is a better material for

	TiO_2		**21.12**			**degradation of MB than $BiVO_4$.**
Reaction Temperature 25 °C	**$BiVO_4$**		**19.66**			**$BiVO_4$ is a better material for degradation of MB than TiO_2**
	TiO_2		**20.05**			

The results of FOM showed that there is a slightly different in FOM average values of BiVO4 (19.6 m.°C /W.hr +/-1.5) and TiO2 (19.5 m.°C /W.hr +/-0.8) to enhance the efficiencies of methylene blue degradation.

3.4. References

1. Pingmuang, K., et al., Composite Photocatalysts Containing BiVO(4) for Degradation of Cationic Dyes. Scientific Reports, 2017. **7**: p. 8929.
2. Sun, J., et al., Novel V2O5/BiVO4/TiO2 Nanocomposites with High Visible-Light-Induced Photocatalytic Activity for the Degradation of Toluene. The Journal of Physical Chemistry C, 2014. **118**(19): p. 10113-10121.
3. ASTM G173-03(2012), Standard Tables for Reference Solar Spectral Irradiances: Direct Normal and Hemispherical on 37° Tilted Surface, ASTM International, West Conshohocken, PA, 2012, www.astm.org.
4. Yunus, W.M. and A.B. Rahman, Refractive index of solutions at high concentrations. Appl Opt, 1988. **27**(16): p. 3341-3.

5. Pingmuang, K., et al., Photocatalytic Mineralization of Organic Acids over Visible-Light-Driven Au/BiVO4 Photocatalyst. International Journal of Photoenergy, 2013. **2013**: p. 7.
6. Rochkind, M., S. Pasternak, and Y. Paz, Using Dyes for Evaluating Photocatalytic Properties: A Critical Review. Molecules, 2015. **20**(1): p. 88.
7. Kasha, M., H. Rawls, and M. Ashraf El-Bayoumi, The exciton model in molecular spectroscopy, Pure Appl. Chem.11, 371-392. Vol. 11. 1965. 371-392.
8. K. Siong, Y., M. Atabaki, and J. Idris, Performance of activated carbon in water filters. 2013.
9. Kumar, K.V., K. Porkodi, and F. Rocha, Langmuir–Hinshelwood kinetics – A theoretical study. Catalysis Communications, 2008. **9**(1): p. 82-84.
10. Khade, G.V., Suwarnkar, M.B., Gavade, N.L. et al. J Mater Sci: Mater Electron (2015) 26: 3309. https://doi.org/10.1007/s10854-015-2832-7
11. Kite, S.V., et al., Nanostructured TiO2 thin films by chemical bath deposition method for high photoelectrochemical performance. Vol. 6. 2018.
12. Gamage McEvoy, J., W. Cui, and Z. Zhang, Degradative and disinfective properties of carbon-doped anatase–rutile TiO2 mixtures under visible light irradiation. Catalysis Today, 2013. **207**: p. 191-199.

13. Kashif, N. and F. Ouyang, Parameters effect on heterogeneous photocatalysed degradation of phenol in aqueous dispersion of TiO2. Journal of Environmental Sciences, 2009. **21**(4): p. 527-533.
14. Pingmuang, Kanlaya, the design and development of novel metal oxide nanocomposites for sunlight driven water cleaning, Doctoral of Philosophy thesis, School of Chemistry
15. Abdellah, M.H., et al., Photocatalytic decolorization of methylene blue using TiO2/UV system enhanced by air sparging. Alexandria Engineering Journal, 2018. 57(4): p. 3727-3735.
16. Klausner, J.F., et al., On the Accurate Determination of Reaction Rate Constants in Batch-Type Solar Photocatalytic Oxidation Facilities. Journal of Solar Energy Engineering, 1994. **116**(1): p. 19-24.
17. Muruganandham, M. and M. Swaminathan, Solar photocatalytic degradation of a reactive azo dye in TiO2-suspension. Solar Energy Materials and Solar Cells, 2004. 81(4): p. 439-457.
18. Lam, S.-M., et al., Degradation of wastewaters containing organic dyes photocatalysed by zinc oxide: A review. Vol. 41. 2012. 131-169.
19. Lea, J. and A.A. Adesina, The photo-oxidative degradation of sodium dodecyl sulphate in aerated aqueous TiO2 suspension. Journal of Photochemistry and Photobiology A: Chemistry, 1998. 118(2): p. 111-122.
20. Coleman, H.M., et al., Degradation of 1,4-dioxane in water using TiO2 based photocatalytic and H2O2/UV processes. Journal of Hazardous Materials, 2007. 146(3): p. 496-501.

21. Ahmadpour, A., et al., Photocatalytic decolorization of methyl orange dye using nano-photocatalysts. Vol. 1. 2015. 121-127.

22. Kumar, A., A Review on the Factors Affecting the Photocatalytic Degradation of Hazardous Materials. Vol. 1. 2017.

23. Zafar, M.N., et al., Effective adsorptive removal of azo dyes over spherical ZnO nanoparticles. Journal of Materials Research and Technology, 2019. 8(1): p. 713-725.

Chapter – 4 -

Conclusion and Prospective work

4.1. **Conclusion:**

In this research, we focused on studying heterogenous photocatalysis of organic dyes in water environment. The first and second investigations ~~was~~ were based on applying titanium dioxide (TiO_2) and bismuth vanadate ($BiVO_4$) photocatalysts due to promising photoactivities in this field. The photocatalytic performance was examined towards targeted dye called MB as model dye using solar simulator equipment. Our developed study also included investigating the effect of different parameters that have significant impact on photodegradation reaction known as reactor volume, initial concentration of dye, films size and thickness, and reaction temperature.

Experiments were carried out and obtained results and discussions were all explained here to show better understanding of photocatalytic performance of the catalysts and comparing the efficiency and effectiveness of each film based on calculated degradation rate of MB. The testing protocol also included applying different parameters, for example, films size and thickness, reactor volume, ~~room~~ reaction temperature, and initial concentration of MB. The obtained figures by varying reaction temperature and films size and thickness reported positive effect on the MB degradation rate (linear relationship, increased value). While varying reactor volume and initial concentration of MB showed negative effect on degradation rate of MB (decreased value).

Comparing results of TiO_2 and that of $BiVO_4$ for every parameter showed that, at varied temperature, $BiVO_4$ film reflected slightly better response compared to TiO_2 film. However, TiO_2 displayed better degradation rate compared to BiVO4 when the reactor volume was varied. In terms of the film

thickness, TiO_2 showed enhanced response compared to $BiVO_4$. For varying film size, TiO_2 indicated better degradation results than $BiVO_4$. At varying light intensity, TiO_2 also exhibited higher degradation rate compared to $BiVO_4$.

4.2. **Prospective work**

In this research, TiO_2 and $BiVO_4$ screen-printed films showed clear and excellent ability for MB degradation at different reaction conditions under solar simulator irradiation. TiO_2 and $BiVO_4$ materials have the potential as good photocatalysts can provide better photocatalytic activity compared to others. In addition, they display good stability in water, simple fabrication methods, and low cost.

The data in this thesis explained that developed films of TiO_2 and $BiVO_4$ photocatalysts can be used for wastewater purification applications. Nevertheless, further work can be made by:

- Create a similar FOM for powder-based photocatalytic water purification systems.
- The Figure of Merit approach may be extended to water splitting and/or CO2 reduction. CO_2 photo-reduction is green technology, cost effective, and ideal for environmental applications using different semiconductors such as TiO_2, SnO_2, and many others. Photocatalytic water splitting, and CO_2 reduction are popular research fields, which can be improve by comparisons between results from different groups.